DOI: 10.1070/RCR4745

Functional materials based on nanocrystalline cellulose

Oleg V. Surov, Marina I. Voronova, Anatoly G. Zakharov

G.A.Krestov Institute of Solution Chemistry of the Russian Academy of Sciences
ul. Akademicheskaya 1, 153045 Ivanovo, Russian Federation

The data on the synthesis of functional materials based on nanocrystalline cellulose (NCC) published over the past 10 years are analyzed. The liquid-crystal properties of NCC suspensions, methods of investigation of NCC suspensions and films, conditions for preserving chiral nematic structure in the NCC films after removal of the solvent and features of templated sol – gel synthesis of functional materials based on NCC are considered.
The bibliography includes 106 references.

Contents

I. Introduction 907
II. Liquid-crystal properties of nanocrystalline cellulose suspensions 909
III. Research techniques for studying nanocrystalline cellulose suspensions and films 914
IV. Conditions for preserving the chiral nematic structure in nanocrystalline cellulose films after solvent removal 919
V. Functional materials obtained by nanocrystalline cellulose-templated sol – gel synthesis 925
VI. Conclusion 931

I. Introduction

In recent years, renewable feedstocks for manufacturing environmentally clean materials have attracted enhanced attention, because of the global climate change and depletion of natural raw material sources. Cellulose is the most abundant natural polymer with an annual production output >75 billion tons.[1] Being a cheap renewable source of biocompatible and biodegradable natural materials, cellulose becomes more and more significant as a feedstock for manufacturing new environmentally clean functional materials.

Cellulose is a polymer, the macromolecules of which are composed of β-D-glucopyranose units linked by 1,4-β-glycosidic bonds into linear chains. The repeating unit of the cellulose polymer chain is a pair of β-D-glucopyranose rings rotated relative to each other (Fig. 1 *a*).

The long and thin nano-sized threads — elementary fibrils — are the primary elements of the supramolecular cellulose structure. The nanofibils of natural cellulose are formed during the biosynthesis in the living cells of plants, algae and some bacteria and animals [crustaceans, snails, tunicates (*Tunicata*, or *Urochordata* — a type of chordata)].[2] The elementary nanofibrils have lateral sizes of 3 – 10 nm, depending on the cellulose origin. According to the amorphous-crystalline model for nanofibril structure,[3,4] cellulose macromolecules are arranged along the fibrils and form alternating areas differing in the degree of ordering — crystalline and amorphous ones (see Fig. 1 *b*). The percentage and the size of crystalline areas depend on the origin of cellulose.

Acid treatment induces selective hydrolysis of the amorphous areas of cellulose, thus releasing nanocrystalline rod-like particles. The product obtained in this way is called nanocrystalline cellulose (NCC) or cellulose nanocrystals (CNC) (see Fig. 1 *b*).

The NCC particles are anisotropic. The sizes of the NCC particles thus obtained vary from 50 to 1160 nm in length and approximately 3 to 50 nm in diameter, depending on the source of cellulose and conditions of hydrolysis[5] (Fig. 2). The aspect ratio (length to the smallest lateral size ratio) is 10 – 30 for NCC isolated from cotton cellulose and ~ 70 for NCC obtained from cellulose produced by animals (tuncin — a sort of cellular tissue isolated from the tunic of tunicates).

For the preparation of NCC, cellulose is hydrolyzed with various mineral acids. Most often, sulfuric[7] and hydrochloric[8] acids are used, or, more rarely, phosphoric acid.[9] However, only controlled hydrolysis with

O.V.Surov. PhD, Senior Researcher at the ISC RAS.
E-mail: ovs@isc-ras.ru
Current research interests: physical chemistry of surface phenomena, self-organization processes, nanomaterials.
M.I.Voronova. PhD, Senior Researcher at the ISC RAS.
E-mail: miv@isc-ras.ru
Current research interests: structure and properties of polymers, nanocrystalline cellulose.
A.G.Zakharov. Doctor of Chemical Sciences, Professor, Head of a Laboratory of the ISC RAS.
Telephone: +7(4932)33 – 6259, e-mail: agz@isc-ras.ru
Current research interests: physical chemistry, solutions, polymers, thermodynamics of polymer – liquid systems, nanoparticles, highly disperse and supramolecular systems.

Received 13 April 2017
Translation: Z.P.Svitanko

© 2017 Russian Academy of Sciences and Turpion Ltd.

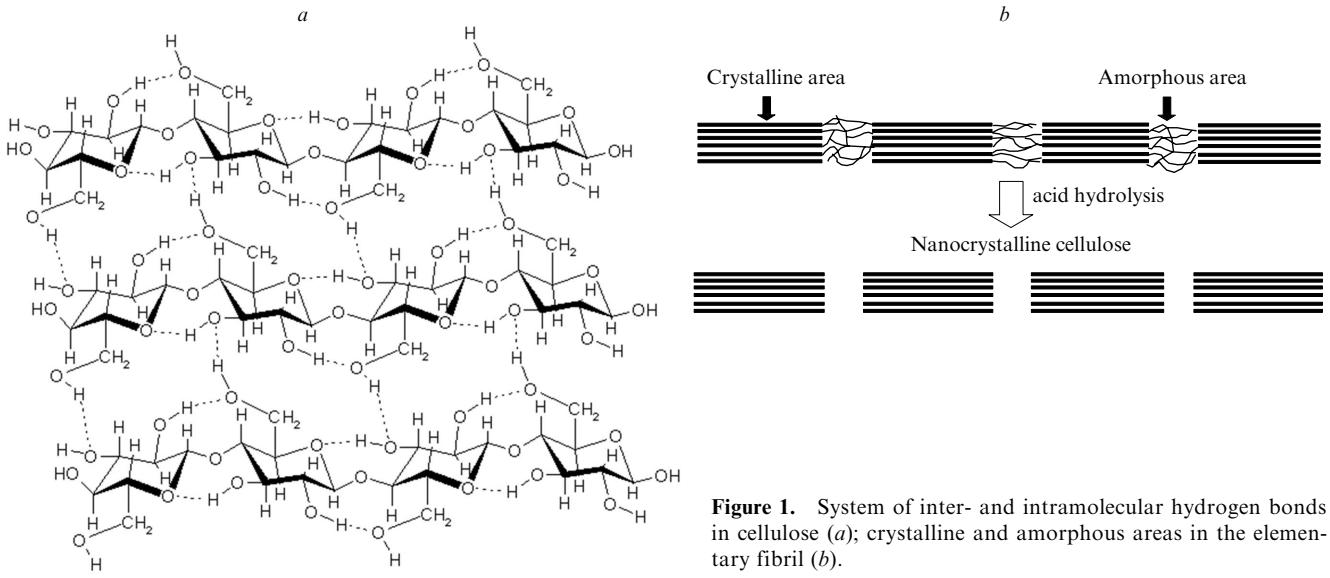


Figure 1. System of inter- and intramolecular hydrogen bonds in cellulose (*a*); crystalline and amorphous areas in the elementary fibril (*b*).

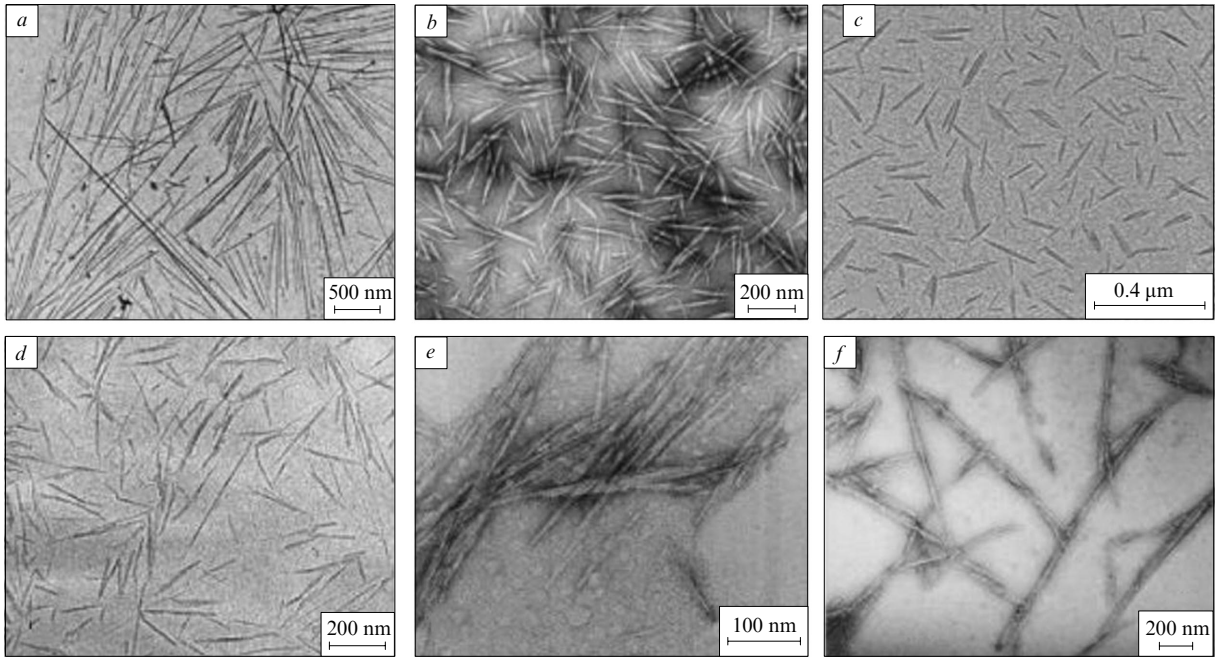


Figure 2. Transmission electron microscopy images of NCC particles obtained by acid hydrolysis of tunicin (*a*), China grass (ramie) (*b*), cotton (*c*), sugar beet (*d*), microcrystalline cellulose (*e*) and bacterial cellulose (*f*).[6]

sulfuric acid[10] makes it possible to graft sulfo groups on the surface of cellulose crystallites (*via* partial esterification of the cellulose hydroxyl groups) and gives rise to stable suspensions, mainly, as a result of electrostatic repulsion between the negatively charged particles.

The preparation and properties of NCC are described in detail in numerous monographs and reviews.[6,11–15] The standard procedure for NCC preparation includes hydrolysis with 62%–65% sulfuric acid at 45–50 °C, removal of the acid using repeated centrifugation, dialysis and sonication cycles. After washing, the dispersion has pH ~2.4 because of the presence of surface OSO_3H groups.[16] Cellulose prepared in this way is called the acidic form of NCC (H-NCC). The neutralization of H-NCC with a 0.1 M NaOH solution to pH 6 affords neutralized NCC form (Na-NCC).

Although the method for isolation of cellulose nanocrystals from microfibrils by treating the cellulose material with an acid was developed for the fist time back in the 1950s by Rånby,[17] the interest in this topic was revived when it was found that an aqueous dispersion of NCC with a particular concentration can form a liquid-crystalline phase.

In 1959, Marchessault *et al.*[18] reported that NCC dispersions obtained by sulfuric acid hydrolysis form lyotropic liquid-crystalline phases. However, the chiral nematic (cholesteric) phase inherent in self-assembled NCC dispersions was not identified until 1992.[10]

In the end of the 1990s, Gray and co-workers[19] demonstrated that a chiral nematic structure can be retained in NCC films upon the evaporation-induced self-assembly (EISA). In this connection, it is noteworthy that self-assembly can take place only in the vicinity of thermodynamic equilibrium, while evaporation only increases the component concentrations in the solution.[20]

The properties of nanocrystalline cellulose — anisotropic particle shape, high surface charge (acquired upon hydrolysis), high mechanical strength,[21] the possibility of chemical modification of the surface hydroxyl groups[22] and the formation of a chiral nematic liquid-crystalline phase in aqueous dispersions and films — attract considerable attention for the design of new functional materials.

According to the SciFinder database, the number of scientific publications dealing with NCC increases every year; especially vigorous growth of the publication activity has been observed in the last 4 – 5 years.[23] Whereas most of early studies addressed the preparation and properties of NCC, currently the majority of publications are devoted to the manufacture of NCC-based functional materials.

II. Liquid-crystal properties of nanocrystalline cellulose suspensions

Owing to their structural features and anisotropic properties, rod-like NCC particles are of considerable interest as building blocks for supramolecular hierarchical structures. However, for these qualities to be manifested in the materials at the macrolevel, it is necessary to clearly understand and control the processes of assembly of large molecular entities.

When sulfuric acid is used for hydrolysis, it reacts with the surface hydroxyl groups of NCC, giving rise to a negative surface charge caused by sulfo groups; this, in turn, promotes complete dispersion of NCC in water because of electrostatic repulsion.[10] Hence, with gradual removal of the aqueous phase, the cellulose nanocrystals would be arranged in such a way as to minimize the existing electrostatic interactions. Indeed, homogeneous concentrated suspensions are self-assembled to liquid-crystalline structures, similarly to what occurs in stable suspensions of other rod-like particles such as polytetrafluoroethylene whiskers, tobacco mosaic virus, DNA fragments or crystallites extracted from polysaccharides, *e.g.* chitin.[12] This self-assembly phenomenon was discovered by observing its characteristic features, pointing to a chiral nematic order, by polarized optical microscopy.[10]

Investigations of these systems demonstrated that NCC crystallites are randomly arranged in a dilute solution forming an isotropic phase. Indeed, polarized optical microscopy shows that at low concentrations of NCC suspensions, the crystallites look like spheroids or ovaloids, while the first ordered domains are similar to tactoids. The nematic liquid-crystal arrangement is formed as the NCC concentration increases as a result of coalescence of these tactoids giving the anisotropic phase, which is characterized by a definite orientation of rod-like NCC particles. When the concentration of the NCC suspension reaches some critical value, an ordered chiral nematic phase is formed, behaving as cholesteric liquid crystals (Fig. 3).[24] Above this critical concentration, aqueous suspensions of NCC exhibit birefringence, and upon storage, they can spontaneously separate into the upper isotropic and lower anisotropic phases (Fig. 4).[25]

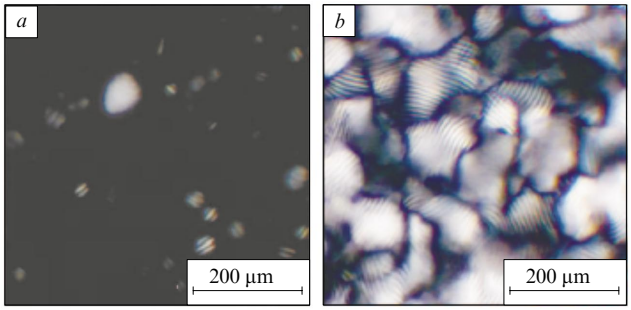


Figure 3. Polarized light images of NCC suspensions.[24] (*a*) Isotropic phase, (*b*) anisotropic phase.

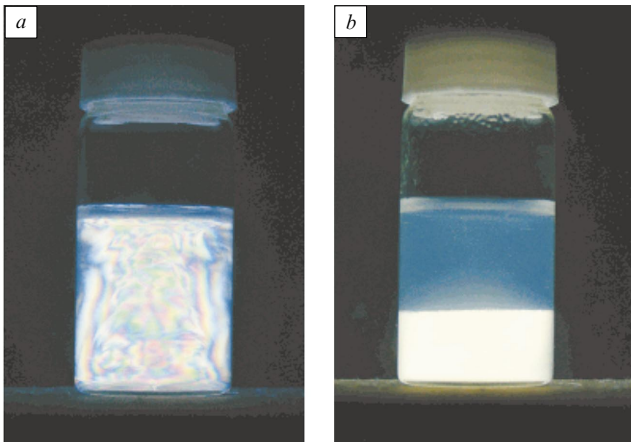


Figure 4. Polarized light images of the aqueous suspension of NCC (0.63 mass %): immediately after mixing, the suspension develops an iridescent colour (*a*); after storage for a week, the suspension is separated into the higher isotropic and lower anisotropic phases (*b*).[25]
In non-polarized light, the suspension looks like a turbid liquid in both cases.

These chiral nematic, or cholesteric, structures in the anisotropic phase consist of planes arranged one above another and formed by rod-like NCC particles stretched in one direction. The direction in which the NCC crystallites are stretched rotates around the axis perpendicular to the plane accommodating the particles from one plane to another, with the helix pitch P, as shown in Fig. 5 *c*. Furthermore, for NCC suspensions and films, only the left-handed chiral structure is formed, unlike the cellulose derivatives, which can form both left- and right-

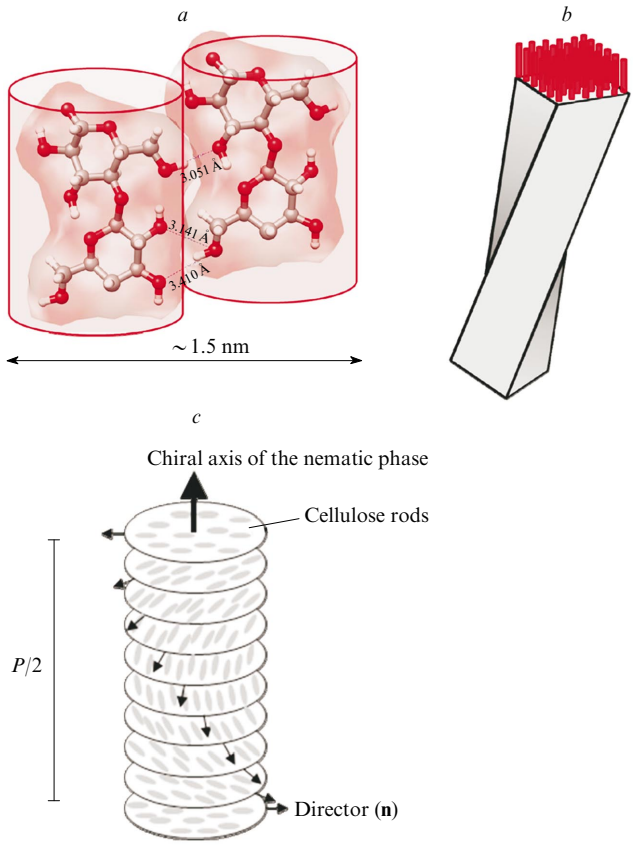


Figure 5. Schematic view of the formation of the left-handed chiral nematic NCC structure: the chirality of NCC suspensions and films is determined by the chirality of carbon atoms of the D-glucoside moieties (*a*), helical morphology of single nanocrystals (*b*) and chirality of lyotropic liquid-crystalline phase (*c*).[26]

handed cholesteric structures.[27] Nanocrystalline cellulose suspensions and films possess three levels of chirality: molecular level resulting from the asymmetric carbon atoms of D-glucoside residues (see Fig. 5 *a*), nanolevel resulting from the twisted morphology of some crystals (see Fig. 5 *b*) and the level resulting from the left-handed chiral nematic long-range order of the lyotropic liquid-crystalline phase.[26, 27]

The spontaneous parallel arrangement of NCC crystallites occurring above a definite critical concentration is well known for an entropy-controlled spontaneous orientation of rod-like particles giving a nematic order. This phenomenon can be interpreted as being due to the positive contribution of the excluded volume interactions, resulting in a higher entropy of the packing compared with that of the disordered phase.

When the $P/2$ value is of the order of several hundred nanometres, a specific Bragg reflection is observed if the light falls approximately along the helix axis. If the helix axis lies in the plane of the specimen, the Bragg reflection is not observed, but when P is about a micrometre or greater, a polarized microscopic examination reveals a characteristic fingerprint texture with repeating bands. The distance between two neighbouring bands is $P/2$ in this case. Thus, a specimen with a cholesteric structure behaves in different ways depending on whether the observation is made along or across the helix axis and on whether the helix pitch is approximately equal to the light wavelength or is much greater.

The liquid-crystalline textures observed through a polarized microscope depend on the orientation of the optical axis of the cholesteric phase relative to the observer. Figure 6 shows a typical image of an aqueous suspension of NCC with planar texture (*A*) and fingerprint texture areas (*B*) in which the chiral nematic plane is parallel and perpendicular to the plane of the specimen, respectively.

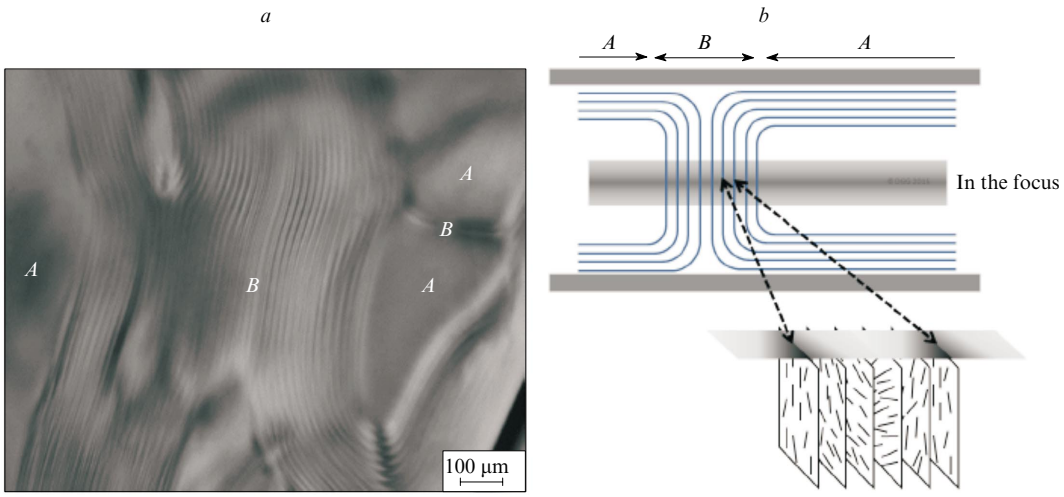


Figure 6. Image of an aqueous suspension of NCC (8 mass %) obtained by polarized microscopy (*a*).[28]
The planar texture (*A*) and the fingerprint texture (*B*) can be seen. Schematic image of the formation of a chiral nematic texture (*b*). Areas *A* and *B* refer to the planar and fingerprint textures, respectively. The optical axis of the polarized microscope is directed from top downward at right angle to the image with the focus being at the centre. The light and dark bands observed through crossed polarizers are due to birefringence, resulting from different orientations of the anisotropic NCC particles along and across the microscope's optical axis.

Presumably, the cause of spontaneous assembly is related to the cause of formation of helical structures, which are often observed in natural materials containing cellulose.[10, 12] Revol and Marchessault[29] hypothesized that NCC particles should be twisted for their chiral interaction. Since suspensions of non-charged NCC particles obtained by hydrolysis in the presence of HCl do not develop such a chiral nematic order, presumably, negative charges of ionized sulfo groups on the surface of NCC particles are necessary for phase stability and the helical arrangement of NCC particles is probably a consequence of this twisting.[10]

In addition, it was found that even if the electrostatic repulsion is shielded by adsorption of surfactants or by grafting of a polymer on the NCC particle surface, NCC suspensions preserve the chiral nematic order.[30, 31] Orts *et al.*,[32] who studied small-angle neutron scattering in aqueous suspensions of NCC upon application of a magnetic field and shear flow, confirmed the hypothesis of NCC particles as helically twisted rods (Fig. 7).

A more weighty piece of evidence was reported by Araki and Kuga,[25] who demonstrated that NCC particles derived from bacterial cellulose form a nematic (achiral) phase in an electrolyte-free suspension, whereas in the presence of an electrolyte, the suspension shows a chiral nematic order. This phenomenon is attributable to morphological changes in the cellulose nanocrystals, which are caused by shielding of the surface charge and transform the cylinder into a twisted rod (Fig. 8). Actually, stretching of NCC particles caused by repulsion of surface charges is expected to hide the chiral morphology by making the rods straight and smooth, which gives rise to a nematic phase with parallel packing of these rods. The addition of an electrolyte should induce a decrease in the effective size of particles; in this case, the twisted morphology results in such an arrangement of rods that gives rise to a chiral nematic order.

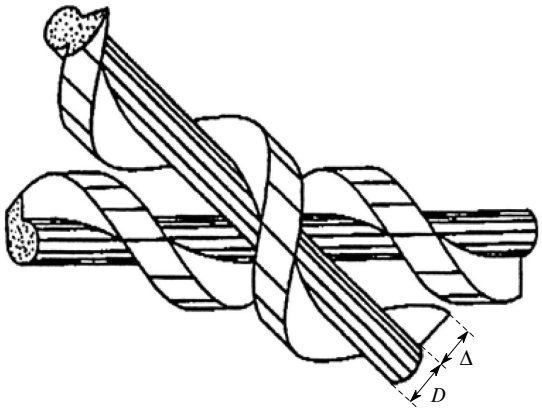


Figure 7. Schematic image of the denser packing attained by chiral interaction of the twisted rods.[32]
The distances between the rods decreases by Δ down to *D* if they do not form a packing with parallel axes, but are packed in such a way that the 'thread' of one rod fits into the 'groove' of the neighbouring rod; the twisted rod is surrounded by the electrical double layer and governs the packing at rather large distances.

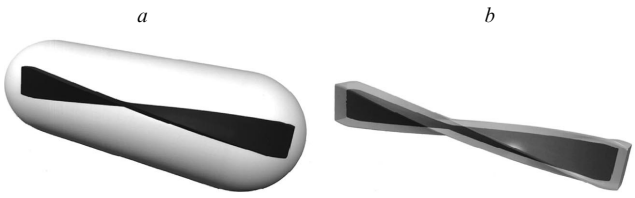


Figure 8. Schematic image of bacterial cellulose nanocrystals with different surface charges demonstrating the change in the particle effective shape.[25]
In water, the surface charge repulsion is long-range, resulting in the apparent achirality of the rod (*a*); addition of NaCl decreases the distance of action of the electrostatic repulsion; as a result, the particle behaves as a twisted rod (*b*).

The concept of ordered chiral nematic phases with properties observed for NCC suspensions corresponds to classical phase equilibrium theories such as the Onsager theory and its extended SLO (Stroobants, Lekkerkerker and Odijk) version: the possibility of formation of a liquid-crystalline phase depends on the particle aspect ratio, surface charge density and osmotic pressure.[33, 34]

According to the Onsager theory, the spontaneous formation of liquid-crystalline phases is due to the fact that the entropy gain upon the translational motion of a rod-like particle in an isotropic medium exceeds the entropy of orientational and rotational motion of particles in an anisotropic medium. As applied to the nematic phase, this means that the translational motion of rod-like particles is more difficult in the disordered state (the particles collide with one another) than in the ordered state (the particles move in parallel). In terms of the original Onsager theory for monodisperse cylinders with the assumption of only elastic interactions between the particles, the liquid-crystalline phase starts to appear at the concentration $\phi_I = 3.3/(L/D)$, while at the concentration $\phi_N = 4.5/(L/D)$, the phase is completely liquid-crystalline (nematic); here ϕ is the volume fraction of rod-like particles in solution, L and D are the particle length and diameter. Thus, the greater the L/D ratio for the particle, the lower the concentration required to attain the liquid-crystalline state.

Since most of real systems are polydisperse and involve complex interactions, there are numerous modifications of this theory to take into account the polydispersity and interactions with the solvent. As a rule, the solvent and polydispersity effects expand the two-phase area.

Stroobants, Lekkerkerker and Odijk modified the Onsager theory by introducing two factors that take into account the increase in the effective diameter of rod-like particles in solution and twisting of particles as a result of electrostatic repulsion. The first application of the SLO theory for describing the phase behaviour of aqueous suspensions of NCC was reported by Gray and co-workers.[34]

Figure 9 shows the volume fraction of the anisotropic phase (with the assumption of nematic phase formation) (ϕ_N) as a function of the total NCC concentration.[35] In the Figure, the two-phase area is located between the concentrations C_1 (the concentration of transition

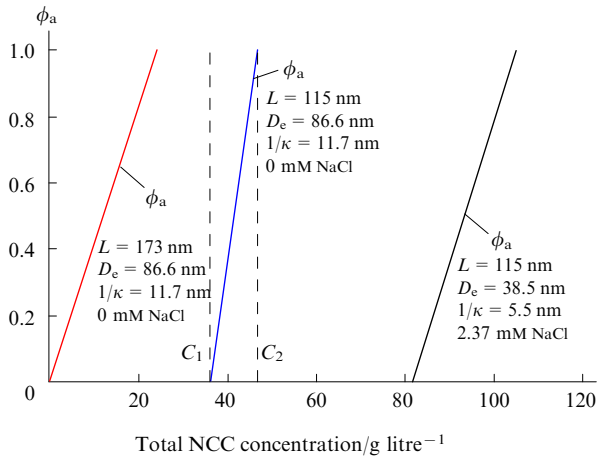


Figure 9. Phase behaviour of NCC predicted by the SLO theory.[35] ϕ_a is the volume fraction of the anisotropic phase, D_e is the effective diameter of the nanocrystal, $1/\kappa$ is the electrical double layer thickness.

between the anisotropic phase and the two-phase system) and C_2 (the concentration at which the isotropic phase disappears). For the middle (blue-coloured) straight line in Fig. 9, the two-phase area (isotropic + anisotropic systems) lies in the narrow concentration range between C_1 = 36 g litre^{-1} and C_2 = 47 g litre^{-1}.

A comparison of the three straight lines in Fig. 9 illustrates the role of variables that control the phase behaviour. The addition of a salt decreases the effective diameter of nanocrystals and thickness of the electrical double layer, which gives rise to the twisted morphology of rod-like NCC particles. As a result, the two-phase area shifts to higher concentrations and expands its borders (black straight line). The SLO model predicts that a 1.5-fold increase in the particle length (from 115 to 173 nm) would shift the two-phase area towards considerably lower NCC concentrations and would expand the borders of the two-phase area (red straight line).

Figure 10 presents the experimental data obtained by different authors and illustrating the phase behaviour of suspensions of various NCC specimens. The specimens differ in the initial feedstock, types of treatment or electrolyte additives used.

Comparison of Figs 9 and 10 shows (taking account of the dimension of NCC concentration) that the SLO theory adequately describes experimental data. The liquid-crystal properties of NCC suspensions in the concentration range >10 mass % – 15 mass % remain largely unexplored, because gelation at high concentrations hampers the studies of equilibrium phases.

The critical concentration of sulfated NCC particles needed for the formation of nematic phases in aqueous suspensions in the absence of an electrolyte depends, to a considerable extent, on the surface charge density and usually varies from 1 mass % to 10 mass %. The helix pitch of the resulting chiral nematic anisotropic phases usually decreases with increasing concentration of the NCC suspensions and varies from 20 to 80 μm.[12]

The isotropic – anisotropic phase equilibrium is sensitive to the presence of electrolytes and the nature of their

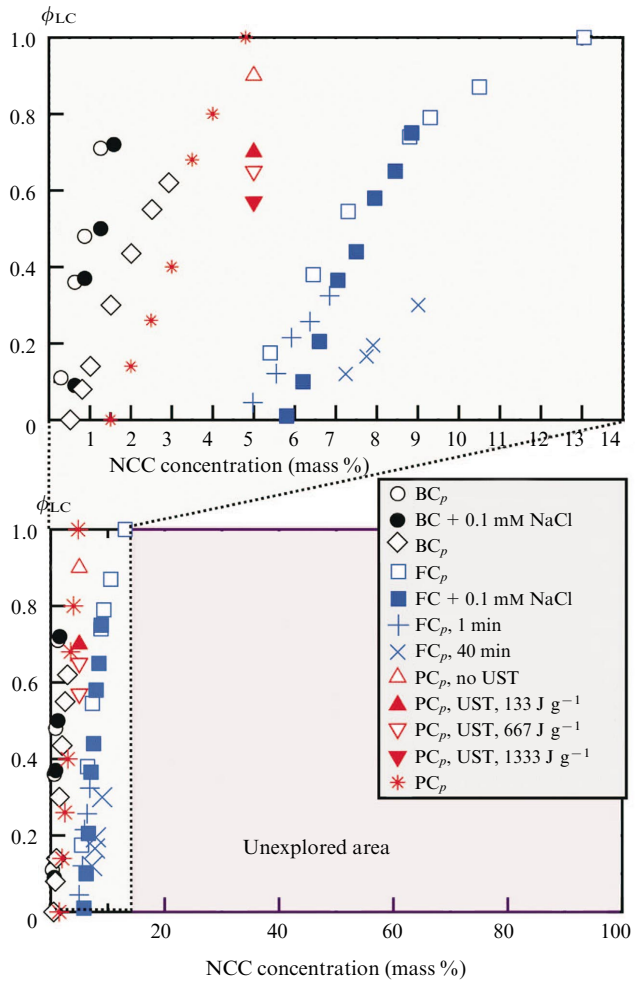


Figure 10. Phase behaviour of NCC suspensions.[24] The abbreviations BC, FC and PC in the plot designate NCC derived from bacterial cellulose, filter paper and fresh wood pulp, respectively. The subscript p stands for pure NCC without any additives; the duration (min) and power (J g^{-1}) of the ultrasound treatment are given.

counter-ions.[36] An increase in the amount of the electrolyte added decreases the formation of the anisotropic phase. It is of interest that the helix pitch of the chiral nematic phase decreases, *i.e.*, the helix becomes more twisted, with increasing electrolyte concentration. Probably, a decrease in the pitch of the helix is caused by the fact that a decrease in the electrical double layer thickness enhances the chiral interactions between the nanocrystallites.[34] For inorganic counter-ions, the critical concentration for the formation of the ordered phase generally increases with increasing van der Waals radius in the series $H^+ < Na^+ < K^+ < Cs^+$. For organic counter-ions such as NH_4^+, Me_4N^+, Et_4N^+, $Pr^n_4N^+$, $Bu^n_4N^+$, Me_3HN^+ and Et_3HN^+, the critical concentration depends on the relative contributions of the hydrophobic attraction and steric repulsion. Generally speaking, most of studies in this field demonstrate that the critical concentration increases with increasing counter-ion size. The chemical nature of the counter-ion also affects the colloidal stability, the temperature dependence of phase

separation, the pitch of the chiral nematic helix and the repeated dispersibility of the dried specimens obtained from suspensions.

Macromolecules such as blue dextran or anionic dyes, which are not adsorbed on NCC, affect the phase separation of aqueous NCC suspensions, which are obtained by sulfuric acid hydrolysis, in the same way as electrolytes.[37–39] However, anionic dyes induce phase separation at a much lower ionic strength than simple (1 : 1) inorganic electrolytes (*e.g.*, NaCl), probably, due to their multiple charge and greater hydration radius. Nevertheless, electrostatic attraction and chemical binding of cationic and anionic dyes are likely to prevent the phase separation in aqueous suspensions of NCC.[37] When the ionic dyes are bound to non-adsorbable macromolecules such as dextran, three-phase equilibrium is observed: isotropic–isotropic–nematic phase. In this case, prolonged settling of NCC suspensions in the presence of a polymer and a dye gives rise to three layers occurring in equilibrium: the upper dye-saturated isotropic layer with a low NCC concentration; the middle isotropic layer with an enhanced NCC concentration; and a lower one in which the NCC particles form a nematic phase. This peculiar behaviour is also observed in the case of neutral blue dextran. The concentration of dextran required to attain the three-phase equilibrium depends considerably on its molecular mass and charge density.[38] The phase behaviour of these suspensions is probably controlled by both the repulsive electrostatic forces and attractive entropy forces. The presence of ionic dyes increases the ionic strength of the system. When the ionic strength is low, a large number of NCC particles is required to attain the critical concentration needed for phase separation; this shifts the phase equilibrium towards the area of coexistence of the isotropic and chiral nematic phases. At a higher ionic strength of the solution, the electrostatic repulsion between the rod-like NCC particles is considerably shielded; hence, the attractive interactions of dextran macromolecules can be manifested and induce phase separation.[39]

The charge nature and charge density on the surface of NCC particles affect the formation of the chiral nematic phase. The NCC specimens obtained by hydrolysis in the presence of HCl and then sulfated contain approximately three times less sulfur than the specimens obtained by hydrolysis directly in the presence of H_2SO_4.[40] The suspensions sulfated in the second stage form a glass-like birefringent phase and are characterized by a cross-hatch pattern (Fig. 11 *a*), whereas the fingerprints indicative of a chiral nematic phase are observed for directly sulfated NCC. It is of interest that a highly viscous suspension of post-sulfated NCC does not produce a chiral nematic phase, apparently, because of low surface charge.

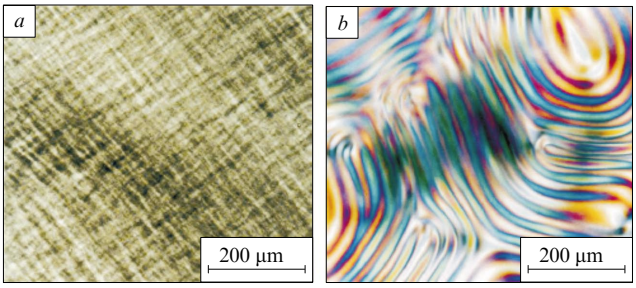


Figure 11. Polarized light photomicrographs of NCC suspensions: reticulate pattern of the post-sulfated suspension (7.1 mass % of solid matter) (*a*); fingerprints of the chiral nematic phase of the suspension obtained directly by sulfuric acid hydrolysis (5.4 mass % of solid matter) (*b*).[40]

A carboxylated NCC obtained by oxidation in the presence of TEMPO (2,2,6,6-tetramethylpiperidine-1-oxyl) forms homogeneous dispersions in water, which exhibit clear-cut birefringence behaviour. However, this feature is not randomly distributed throughout the system; there are domains of different size and colour, which is indicative of a local orientation of domains in the suspension that has not reached chiral nematic order composed of tactoids or fingerprints. The absence of further organization is attributable to higher polydispersity in length (for NCC particles obtained from tunicates by prehydrolysis in the presence of HCl) and high viscosity of the suspension.[41] However, if the carboxylated NCC is prepared from cotton fibre, the length polydispersity of NCC particles decreases and the suspensions reach the chiral nematic order with a helix pitch of 7 μm at a 5 mass % or higher concentration. Furthermore, when a polymer is grafted to the NCC surface, the resulting NCC crystallites form a chiral nematic mesophase as a result of phase separation, similarly to what occurs with non-modified NCC, but with shorter distances between the fingerprint lines (~4 μm).[13] Moreover, as opposed to earlier data, polymer-grafted NCC shows markedly enhanced stability of dispersions even at high contents of the disperse phase and the repeated dispersibility in water or chloroform from the freeze-dried state. These suspensions have a high colloidal stability at high ionic strengths of the solution: no aggregation was detected as the NaCl concentration was increased to 2 mol litre^{-1}.

The epoxypropyltrimethylammonium chloride-grafted NCC suspensions exhibit birefringence, but no phase separation giving the chiral nematic liquid-crystalline phase was detected, probably, because of too high suspension viscosity.[13]

Suspensions of NCC in polar organic solvents also form the chiral nematic liquid-crystalline phase.[42–45] Lagerwall and co-workers[45] have shown that the self-assembly of NCC particles is much faster in solvents with high dielectric constants (DMF, methylformamide, formamide) than in water, with the pitch of the chiral nematic helix being decreased with increasing dielectric constant of the solvent. Viet *et al.*,[42] who studied suspensions of freeze-dried NCC in DMSO and DMF, arrived at the conclusion that a minor amount of water critically affects the suspension stability. Blachechen *et al.*[44] have found that dispersibility of NCC in solvents (DMF, THF, ethyl acetate) increases with increasing dielectric constant. This observation was supported by Okura *et al.*,[43] who studied the dispersibility of NCC in 21 organic solvents.

Heux *et al.*[31] were the first to describe the self-assembly of NCC particles in non-polar solvents. They used a surfactant coating for dispersion of NCC and obtained concentrated NCC suspensions (up to

36 mass %) with a chiral nematic structure. It was found that a helix pitch for this structure equal to ~4 μm is too small compared with that for aqueous suspensions (20 to 80 μm). These results indicate that the steric stabilization induced by the surfactant coating does not 'notice' the electrostatic repulsion and, hence, it induces stronger chiral interactions between rod-like NCC particles, which finally gives rise to a denser packing. The same research group comprehensively studied the relationship between the geometric parameters of the NCC particles extracted from cotton fibre and their behaviour in non-polar solvent dispersions (*e.g.*, in cyclohexane). The critical concentration at which the chiral nematic mesophase spontaneously formed was higher than in water. No quantitative correlation with the Onsager theory was found for these organophilic suspensions: the experimental critical concentration was much lower than that predicted by theory, probably, as a result of mutual attraction between rod-like NCC particles in a non-polar medium, which decreases the pitch of the chiral nematic helix down to <2 μm. In addition, suspensions of NCC nanoparticles with a large aspect ratio do not display any phase separation, but form an anisotropic gel phase at a high concentration.[46] Conversely, in the case of NCC suspensions in toluene stabilized by some polymers, the pitch of the chiral nematic helix can markedly increase (up to ~17 μm).[47]

III. Research techniques for studying nanocrystalline cellulose suspensions and films

The structure and properties of NCC-based materials imply the use of a particular set of specific research methods. The polarized optical microscopy (POM) is the key method for studying both NCC suspensions and films. As a result of formation of the chiral nematic structure, NCC films show photonic properties, which can be spectrally detected over a broad wavelength range, in particular, using circular dichroism spectroscopy. Transmission electron microscopy (TEM), scanning electron microscopy (SEM) and atomic force microscopy (AFM) can be used to determine the pitch of the helix, direction of helix twisting and direction of the axis of the chiral nematic structure for NCC films.

III.1. Polarized optical microscopy and circular dichroism spectroscopy

Polarization of light is a physical characteristics of optical radiation related to the transverse anisotropy of light waves, that is, non-equivalence of various directions in the plane perpendicular to the light beam. The understanding of polarization of light was markedly promoted by its manifestation in interference of light and, in particular, by the fact that two light beams with mutually perpendicular polarization planes do not directly interfere.[48]

The transverse character of electromagnetic waves eliminates the axial symmetry of the wave relative to the propagation direction because of the presence of preferred directions [electric field strength (**E**) and magnetic field strength (**H**) vectors] in the plane perpendicular to the propagation direction. Since the electromagnetic wave vectors **E** and **H** are perpendicular to each other, the behaviour of only one of them needs to be known for the full description of the polarization state of a light beam. Usually vector **E** is chosen for this purpose

Light is called completely polarized if two mutually perpendicular components (projections) of light beam vector **E** execute oscillations with a time-invariable phase difference. Usually, the state of polarized light is depicted by the polarization ellipse — projection of the trajectory of the end of vector **E** on the plane perpendicular to the beam (Fig. 12).[48]

The projection pattern of completely polarized light is, in the general case, an ellipse with right- or left-hand rotation of vector **E** with time (see Fig. 12 *b*,*d*,*f*). Such a light is called elliptically polarized. Of most interest are the limiting cases of elliptical polarization — linear polarization where the polarization ellipse is degenerated into a straight line segment (see Fig. 12 *a*,*e*), defining the position of the polarization plane, and circular polarization where the polarization ellipse is a circle (see Fig. 12 *c*). In the former case, light is called plane or linearly polarized, while in the latter case, it is right- or left-hand circularly polarized, depending on the direction of rotation of vector **E**.

Figure 13 shows the photographs of the chiral nematic NCC structure obtained by a polarized microscope.[24] In Fig. 13 *a*, one can see parallel lines inherent in a

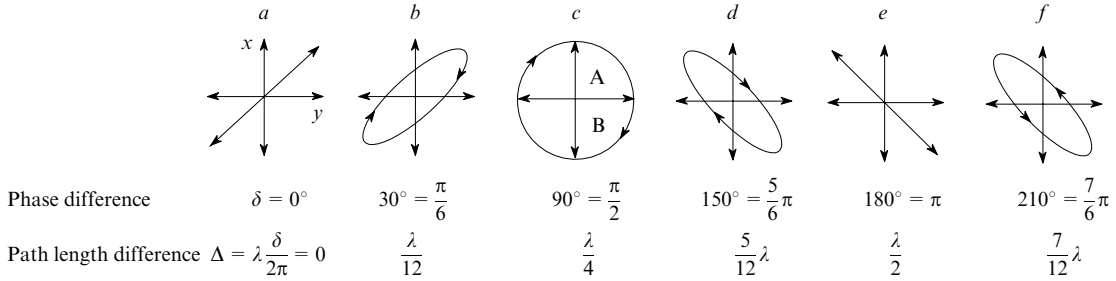


Figure 12. Examples of various types of light beam polarization for different phase differences between the mutually perpendicular components E_x and E_y.[48]
The plane of the drawing is perpendicular to the light propagation direction; *a* and *e* are linear polarization; *c* is circular polarization; *b*, *d*, *f* is elliptical polarization. The schemes correspond to positive phase differences δ (vertical oscillations ahead of horizontal oscillations); λ is the light wavelength.

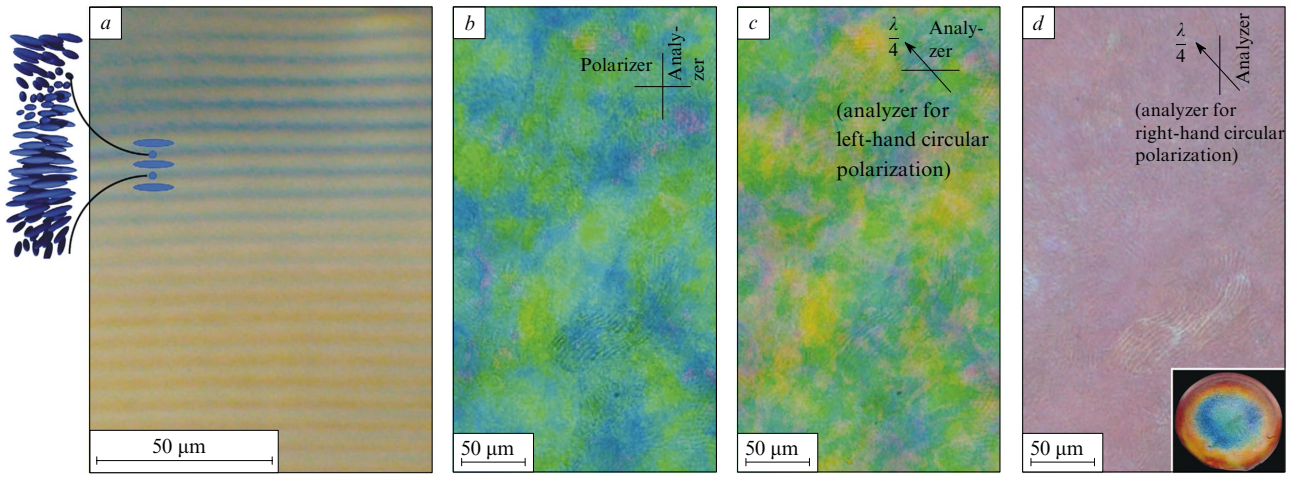


Figure 13. Texture traces of formation of the helical liquid-crystalline structure observed by polarized microscopy.[24] (*a*) 5% aqueous suspension of NCC (transmitted image); (*b* – *d*) dried NCC films (reflected images); (*b*) crossed linear polarizers; (*c*, *d*) the plate shifting the phase by quarter of the wave and position of the polarizer form the analyzer for left- (*c*) and right-hand (*d*) circular polarizations. For inset in Fig. *d*, see the text.

helical structure with the axis lying in the specimen plane (The helix axis is considered to be usually perpendicular to the specimen plane). The distance between the neighbouring lines is equal to half the pitch of the helix ($P/2$), the pitch for this specimen being $P \approx 13$ μm. Figure 13 *b* – *d* presents typical images of the dried NCC films with non-uniform orientation of helices and a large scatter of the pitch P values. The film shown in Fig. 13 *b* is exposed to linearly polarized light and is observed through crossed linear polarizers. The film shown in Fig. 13 *c*,*d* is exposed to non-polarized light and is observed through linear polarizers and a plate shifting the phase by a quarter of the wave, which constitute the analyzer for the left- (*c*) and right-hand (*d*) polarizations, respectively. The inset in Fig. 13 *d* shows the iridescent colouring of the dried NCC film (25 mm in diameter) on the black substrate, which can be seen by the naked eye.

Figure 14 presents one more interesting example of a NCC thin film, the colour of which is dictated by the structure.[49] When observed with the naked eye, the middle of the film is uncoloured, while at the edges of the dish, colour rings ranging from blue to red appear. However, polarized microscope examination indicates that particularly the central part of the film (which appears colourless under the naked eye) has a chiral nematic structure, whereas no this structure is present at the edges. This is related to the so-called 'coffee-stain ring' effect, which causes an increase in the film thickness at the edges in comparison with the centre during solvent evaporation. Thus, the colours observed with the naked eye are determined by light interference in the thin film and depend on the film thickness and illumination angle. The central part of the film is too thin to reflect visible light.

Circular dichroism (Cotton effect) is a special case of elliptical dichroism; the effect is based on different

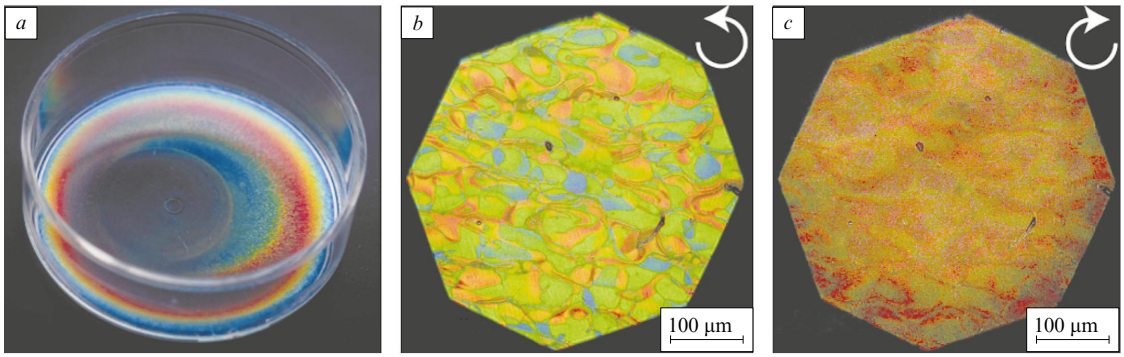


Figure 14. Photograph of a Petri dish with the NCC film obtained from a 4% aqueous suspension by drying under ambient conditions (*a*); polarized microscopy images of the central part of the film demonstrating intense iridescent colour upon reflection of left-hand circularly polarized light (*b*) and dark field upon reflection of right-hand circularly polarized light (*c*).[49]

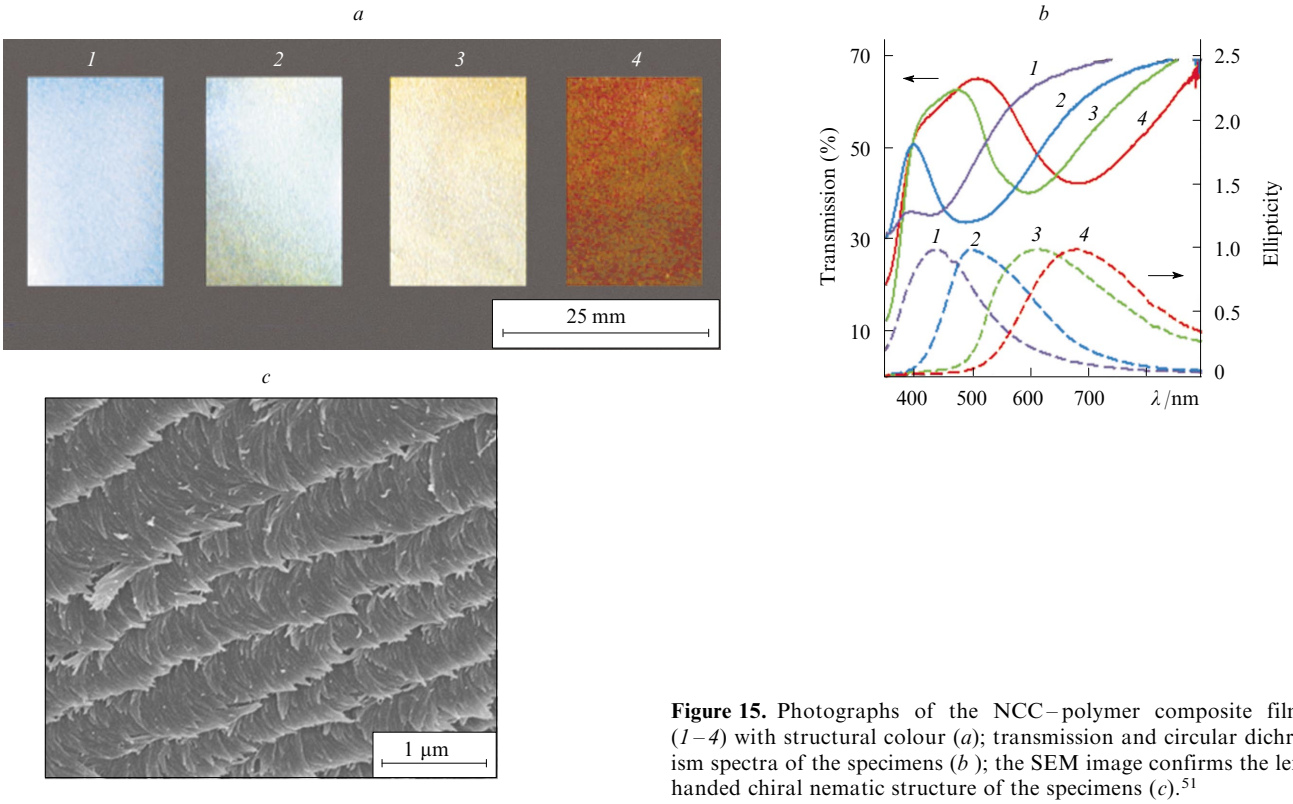


Figure 15. Photographs of the NCC–polymer composite films (*1*–*4*) with structural colour (*a*); transmission and circular dichroism spectra of the specimens (*b*); the SEM image confirms the left-handed chiral nematic structure of the specimens (*c*).[51]

absorption of light with different directions of circular polarization.[50] Thus, circular dichroism is determined by the difference between the absorbances of left-hand and right-hand circularly polarized light

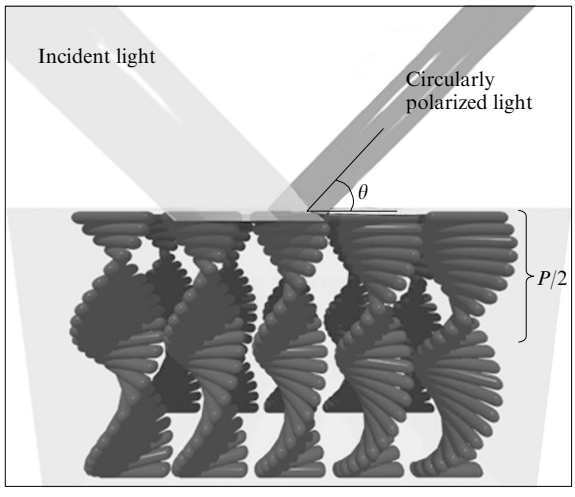
$$\mathrm{CD} = A_\mathrm{L} - A_\mathrm{R} \qquad (1)$$

where A_L is the absorbance for left-hand circularly polarized light and A_R is the absorbance for right-hand circularly polarized light. The apparent absorbance can also be a consequence of reflection of circularly polarized light by chiral nematic liquid-crystalline phases or films. If a chiral specimen predominantly reflects left-hand circularly polarized light, the intensity of light that has passed through the specimen decreases, which leads to seeming absorption of left-hand rather than right-hand circularly polarized light. In this case, the CD signal is positive and indicative of a left-handed helical structure. Conversely, the right-handed helical structure gives rise to a negative CD signal. For chiral specimens reflecting the visible light, the sign of the CD signal resulting from reflection of circularly polarized light is indicative of the direction of rotation of the helical structure.

Figure 15 shows the photographs of the NCC-based chiral composite films and the transmission and circular dichroism spectra. A positive CD signal is indicative of a left-handed chiral structure, which is confirmed by the SEM image.[51]

The interference colours of NCC films observed with a polarized microscope are due to birefringence. The light interference is caused by the phase shift associated with different refractive indices for polarizations along and across the rod-like NCC particles. It is important that the colour of the film can be seen by the naked eye without light polarizers, but it is caused by a reason other than birefringence-induced interference.

A possible source of the colour of NCC films is the formation of structures with a photonic band gap. A very important characteristic of optical properties is the organization type of the periodic structure (1D, 2D,



$$\lambda_\mathrm{max} = n_\mathrm{avg} P \sin\theta$$

Figure 16. Selective reflection of the circularly polarized light by the chiral nematic structure of the NCC film.[20]
The rods show the orientation of the unit vector **n**, which is parallel to the film surface and rotates together with the chiral helix.

3D), meaning the number of directions in which the incident light flux can vary. If there are one or two directions, this is a diffraction grating; if there are three directions, it is a bulk structure or a photonic crystal. Owing to the periodic change of the refractive index, photonic crystals can have allowed bands and band gaps for the photon energies, similar to the allowed bands and band gaps for the energies of charge carriers existing in semiconductors. Practically, this means that if a photon incident on a photonic crystal has an energy (wavelength, frequency) that corresponds to the band gap of this photonic crystal, then the photon cannot propagate in the crystal and is reflected back. Conversely, if the energy (wavelength, frequency) of the incident photon corresponds to an allowed band of this photonic crystal, then it can propagate in the crystal. In other words, the photonic crystal functions as an optical filter, and particularly this feature accounts for the colour of the NCC films with a chiral nematic structure, provided that the pitch of the chiral helix (P) is of the same order of magnitude as the light wavelength (λ) and the incident angle (θ) can be taken to be 90°. The periodicity of the structure gives rise to a Bragg reflection in a narrow range of wavelengths; this produces a strong colour, which does not depend on the film thickness. In this case, according to the equation

$$\lambda_{max} = n_{avg} P \sin\theta \quad (2)$$

where λ_{max} is the wavelength corresponding to the maximum intensity of the reflected light; n_{avg} is the average refractive index; P is the pitch of the cholesteric structure; and θ is the reflection angle, the iridescent colouring depends on both the pitch of the helix and the observation angle (Fig. 16).[20]

As a result of appearance of the helical structure, the reflected light becomes circularly polarized, with the light polarization plane rotating in the same direction as that in the chiral film. A simple method for checking whether the colouring is a consequence of the helical arrangement of NCC particles is to observe the specimen using left- and right-handed circular polarizers. The latter should suppress the colour because NCC forms a left-handed helix. It is noteworthy that a Bragg reflection does not arise if the incident light is perpendicular to the helix axis, even if P falls in the required range. From the practical standpoint, this means that the axis of the helix should be mainly located at right angle to the specimen plane.

In this connection, it should be noted that, as indicated by some authors, the structural colouring of NCC films cannot be attributed to the helical structure alone, because the pitch of the helix is usually too large for the Bragg reflection of visible wavelengths to occur. A possible explanation is the formation of the smectic liquid-crystalline phase. In this case, the photonic structure is determined by the smectic planes, which are indeed spaced by hundreds of nanometres apart.[42] Probably, the existence of a smectic phase forming a helix (chiral smectic phase) is theoretically possible.

III.2. Transmission electron microscopy and scanning electron microscopy

The chiral nematic structure formed upon self-assembly of anisotropic NCC particles in aqueous suspensions is partially preserved in the film after evaporation of water. However, the arrangement of rod-like nanoparticles can be disrupted upon changes in the volume, ionic strength and surface area during evaporation and under the action of convective forces, which affect the morphology and optical properties of the dried films. Practical application of chiral nematic materials implies that exhaustive information on their structure is available.

The data gained by TEM indicate that in the case of a uniform planar texture with the axis of the cholesteric helix being perpendicular to the film surface, the fracture cross-section demonstrates a quasi-layered structure; the thickness of the layer is determined by the helix pitch. If the film cross-section is made at an oblique angle to the cholesteric phase axis, arching is observed (Fig. 17), the

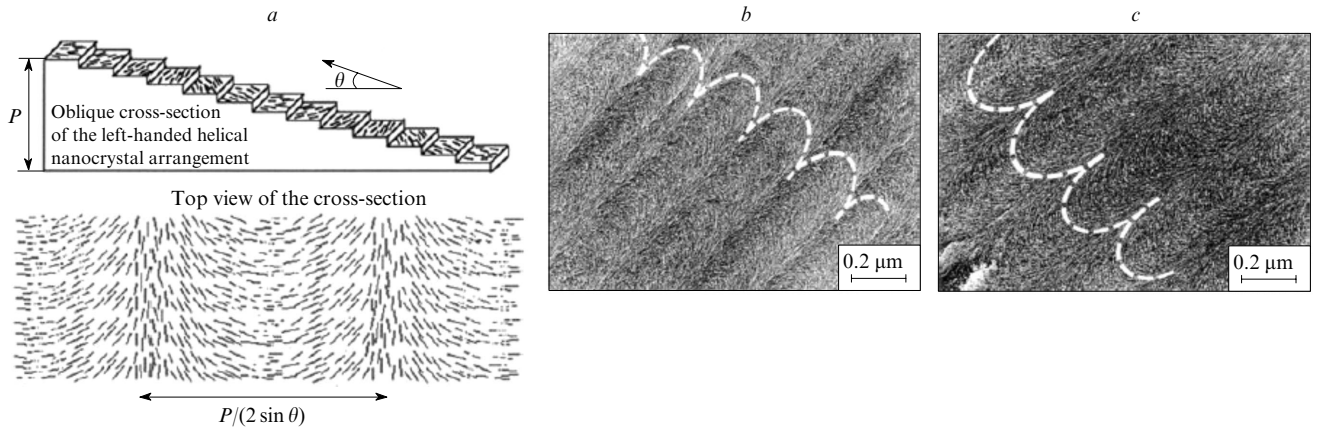


Figure 17. Schematic TEM image (below) of the cross-section of the film (with a planar chiral nematic structure) at some oblique angle (above) (*a*).[26]
The oblique cross-section of the film gives rise to arching. Arches observed in the TEM images of oblique cross-sections of chiral nematic NCC films. The cross-section thickness is 70 nm. The cross-sections are made at such an angle that the upper left-hand corner of the image is inclined towards the observer (*b*) and away from the observer (*c*).

shape of the arches being dependent on the angle between the chiral axis and the cross-section of the film and on whether the helix is left- or right-handed.[26]

The arched patterns observed in the TEM images of the oblique cross-sections of the planar chiral nematic NCC films are indicative of a left-handed helical structure. However, this procedure requires a very delicate specimen preparation and image processing.

Scanning electron microscopy is distinguished by simple specimen preparation and easy visualization of fracture cross-sections of films at high resolution.

When an NCC film is examined with an optical microscope in the transmission mode between crossed polarizers (Fig. 18 *a*), it shows a usual multidomain structure, because the direction of the chiral nematic axis is not invariable, but changes randomly in various sites of the film. In some sites, fingerprint textures are seen, which are characteristic of the case in which the chiral nematic axis is perpendicular to the observer (parallel to the plane of the film). The distance between the fingerprint texture lines is equal to the half of the cholesteric helix pitch. In Fig. 18 *a*, the $P/2$ value is $\sim 1-3$ μm. The image also shows more diffuse and wider lines inherent in structures with the cholesteric axis being arranged at an oblique angle to the film surface. The colours observed in the polarized light are caused by interference induced by birefringence of anisotropic NCC nanocrystals.

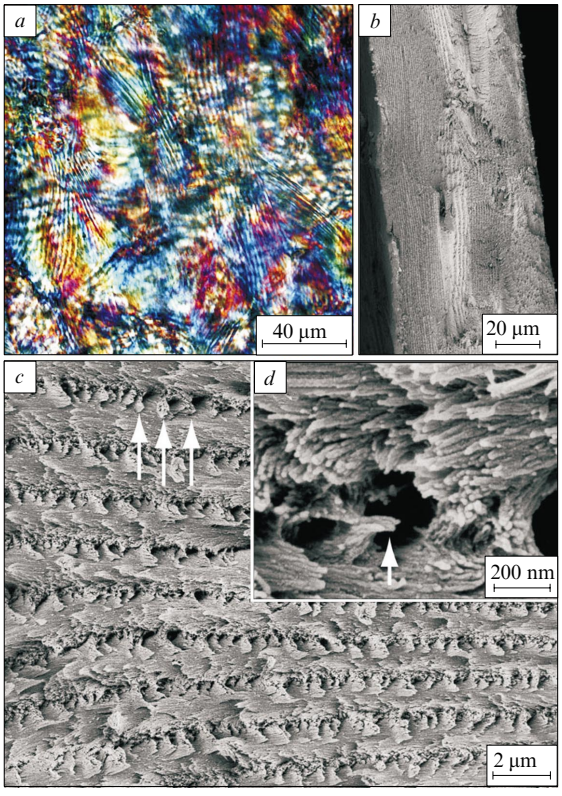


Figure 18. Optical polarized microscopy image (crossed polarizers) of the NCC film surface (*a*); SEM images of the fracture cross-section of the film (*b*–*d*).[26]
The white arrows in Fig. *c*, *d* point to nanocrystal bundles protruding above the fracture surface.

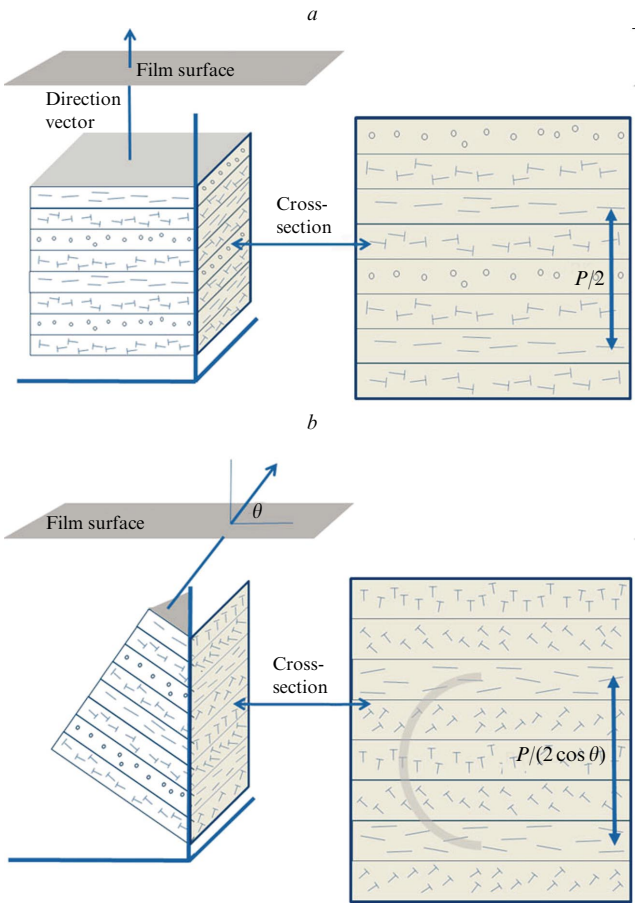


Figure 19. Cross-section of the left-handed chiral nematic structure.[26]
(*a*) Planar texture, the helix axis is perpendicular to the film surface; (*b*) the helix axis is inclined relative to the film surface.

A SEM image of the film cross-section is shown in Fig. 18 *b*. The direction of the chiral nematic helix across the film thickness varies in an arbitrary way. An extended area with a regular arrangement of fingerprint texture lines can be seen in the left part of the image. This indicates that the cholesteric axis is nearly perpendicular to the film surface and the distance between the lines, equal to $P/2$, is ~ 1 μm, which is in good agreement with the value derived from optical microscopic examination. Areas of more diffuse fingerprint lines, in which the cholesteric helix is arranged at an oblique angle to the fracture surface, are also present.

Figure 18 *c*,*d* shows a larger magnification for the layered structure in which the orientation of single nanocrystals can be clearly seen. The fan-like appearance of the structure corresponds to the left-handed arrangement of nanocrystals with the axis running from top to bottom. A distinctive feature of the SEM images in Fig. 18 *c*,*d* is a developed porous structure clearly seen between the layers in the film cross-section.

The fan-like pattern presented in Fig. 18 *c* resembles the arched pattern shown in Fig. 17 with the only differ-

ence that in the former case, the axis of the chiral nematic structure is arranged at an angle to the fracture surface of the film. This case is illustrated in Fig. 19, which shows a plane projection of the spatial arrangement of nanocrystals (for clarity, the nanocrystals are depicted as nail-like items).

For a left-handed structure, the nail heads are oriented away from the observer (see Fig. 19 *b*). If the film cross-section is parallel to the chiral nematic axis, no arched pattern is observed (see Fig. 19 *a*). In the case of cholesteric axis oriented at an oblique angle to the fracture surface, the C-shaped arched pattern appears (see Fig. 19 *b*); when the axis deviates from the fracture surface, a D-shaped pattern can be seen.

Thus, interpretation of the fan-like texture of the film fracture observed by SEM is in line with the views on the chiral nematic structure.

Figure 20 shows the detailed interpretation of the SEM image of the NCC film fracture.

As shown in Fig. 20, line *DE* runs along the projection of the chiral nematic axis on the fracture surface. Proceeding from the orientation of nanocrystals protruding above the plane (for clarity, they are depicted as nail-like items), the left-handed helix is formed. By analogy with the arches observed by TEM (see Fig. 17), the D-shaped circular arches *AB* and *AC* indicate that the chiral nematic axis is projected on line *DE* in such a way that the axis is more remote from the surface at point *E* than at point *D*.

Thus, TEM and SEM studies of the fracture cross-section of NCC film reveal a regular fan-like pattern typical of the cross-section of the left-handed cholesteric helix. Using SEM, it is possible to determine the helix pitch and the helix direction and distinguish between the right- and left-handed helices. In addition, it was found that the chiral nematic structure of the film possesses a regular porosity.

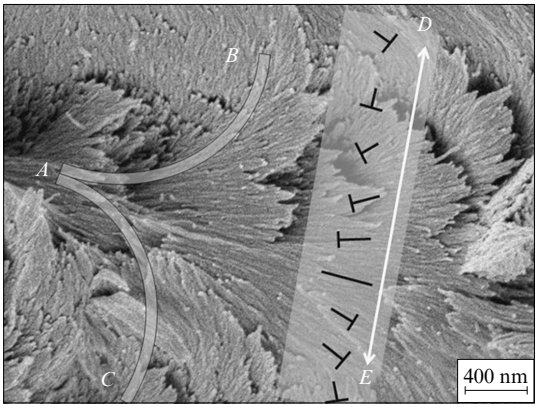


Figure 20. Interpretation of the SEM image of the NCC film fracture.[26]
Line *DE* shows the projection of the chiral nematic axis on the fracture plane. The orientation of nanocrystals outside the fracture plane is shown by nail-like items whose tips indicate the projection above the plane. The observed arches *AB* and *AC* are due to deviation of the chiral nematic axis from the fracture plane.

IV. Conditions for preserving the chiral nematic structure in nanocrystalline cellulose films after solvent removal

The self-assembly of NCC suspensions giving helical structures and preservation of the chiral order in NCC films after removal of the solvent account for the enormous potential of NCC for the development of new materials with valuable optical and mechanical properties. The pitch of the left-handed chiral helix in NCC films can vary approximately from 1 to 50 μm, depending on the size and concentration of NCC nanoparticles, pH, ionic strength of the solution, temperature and so on. Many aspects of formation of the chiral helix are not entirely clear; this restricts the possibility to control the pitch size, which is required, in particular, for studying materials with controlled optical properties. It is necessary to establish the direct relationship between the chiral structure in the liquid-crystalline suspension and the chiral structure in the dried film. If the liquid-crystalline structure is formed under equilibrium (provided that there is sufficient time), the chiral structure in the film is often difficult to control, because self-assembly can occur only under conditions close to thermodynamic equilibrium and evaporation only increases the concentration of components in the solution.[20]

Revol *et al.*[19] used the ability of NCC suspensions to undergo the lyotropic chiral nematic ordering, giving rise to iridescent solid cellulose films with unique controlled optical properties, merely upon controlled evaporation of water from suspensions on a planar surface. The liquid-crystalline order inherent in suspensions is preserved in solid films and the pitch of the chiral nematic helix in dried films is of the same order of magnitude as the visible light wavelength. This unique system was described as an interference device able to reflect circularly polarized light in a definite wavelength range. Since the reflected wavelength determines the spectral colour of light, the perceived colour of the film depends on the helix pitch of the cholesteric structure and on the light incidence angle. The microstructure of these films is very

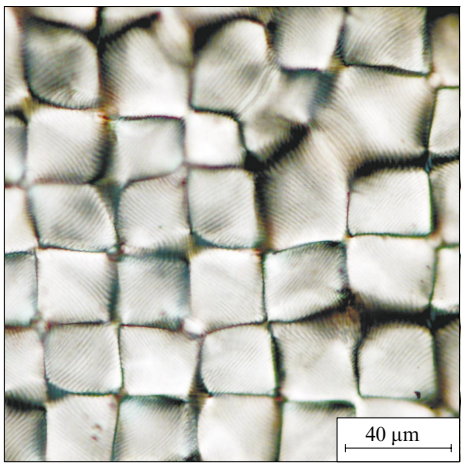


Figure 21. Image of NCC film obtained by a polarized optical microscope between crossed polarizers.[52]

sensitive to drying conditions. Moreover, the perceived colour of the reflected polarized light is controllable, since the ultimate pitch of the helix can vary depending on a number of variables such as the aspect ratio of the rod-like NCC particles and the content of electrolyte. The films prepared under ambient conditions usually demonstrate a multidomain structure, with the helical axes of various chiral nematic domains pointing to different directions. Actually, Roman and Gray [52] were the first to publish compelling evidence for the fact that a parabolic focal conic structure (the symmetrical form of the focal conic defects in which linear defects are formed from pairs of perpendicular, antiparallel and confocal parabolas) is incorporated into self-assembled solid NCC films (Fig. 21).

Gray [53] analyzed in detail the formation of NCC films upon evaporation of water from a dilute aqueous NCC suspension. He demonstrated that concentrating the suspension followed by the formation of films includes several successive stages.

1. Dilute isotropic suspension with a moderate viscosity in which NCC particles are stabilized by the surface sulfonic or carboxyl groups (concentration range from 0 to C_a in Fig. 22).

2. As the concentration of NCC increases, an ordered chiral nematic phase starts to form. The liquid-crystalline phase often appears initially as so-called tactoids, *i.e.*, drops of the anisotropic phase surrounded by the isotropic medium. The pitch of the chiral nematic helix in this two-phase medium almost does not change (segment AB in Fig. 22).

3. Further increrase in the NCC concentration entails an increase in the viscosity of the suspension. The suspension becomes anisotropic; the helix pitch monotonically decreases with increasing NCC concentration (segment BC').

4. Further increase in the concentration of the suspension induces gelation, which prevents further decrease in P (segment $C'D'$).

5. Dehydration of the gel during further evaporation of water may result in 'freezing' of the chiral nematic structure in the glassy state (segment $D'E$).

The above-listed stages are shown in Fig. 22. The pitch of the cholesteric helix of the dried film depends on the particular segment of the whole pathway AE in which the film structure was fixed.

A large aspect ratio of the rod-like NCC particles is favourable for both the formation of liquid-crystalline phases and gelation. In practice, both phenomena can occur simultaneously with increasing concentration of NCC suspensions; most often, liquid-crystalline phases are formed initially, while gelation takes place at higher concentrations. The liquid-crystal properties of NCC dispersions with concentrations >10 mass % – 15 mass % remain largely unexplored, because gelation at high concentrations considerably hampers investigation of equilibrium phases. Presumably, gelation is the main cause of the absence of higher-order liquid-crystalline structures

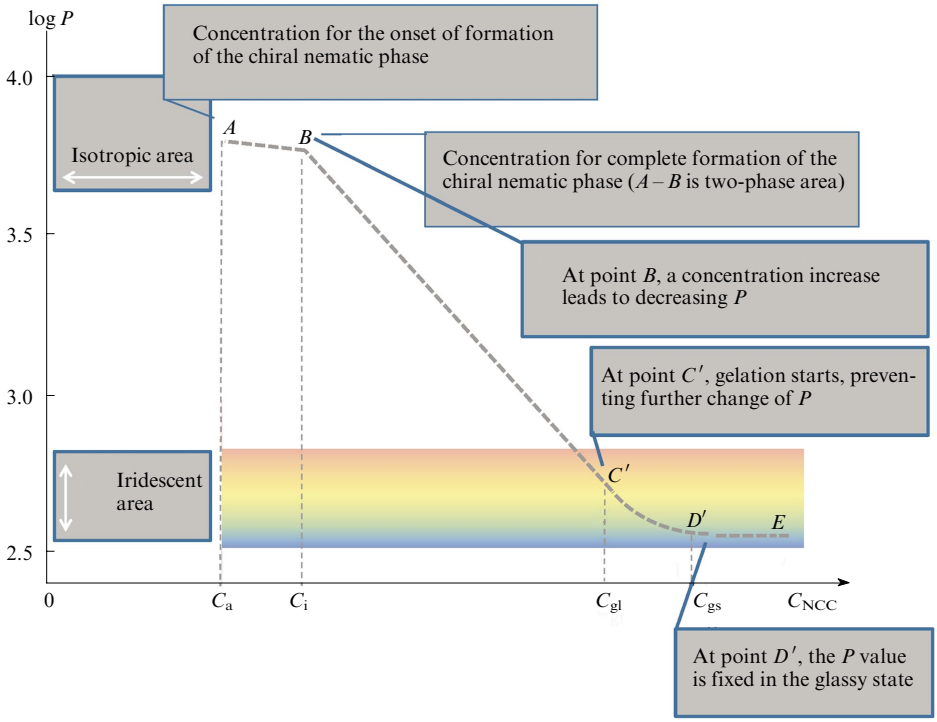


Figure 22. Illustration of the observed dependence of the pitch of the chiral nematic helix on the NCC concentration (C_{NCC}) during water evaporation and film formation.[53]
The iridescent area ($\log P \sim 2.6-2.8$) reflects the range of P corresponding to visible light wavelengths. The concentrations C_a and C_i are the critical NCC concentrations for the onset and completion of formation of the chiral nematic phase; C_{gl} and C_{gs} are the gelation and glassy state formation concentrations, respectively.

(*e.g.*, smectic) and of the high structural diversity of films obtained by drying NCC suspensions.[24]

Because of the presence of the surface charge determined by sulfuric acid esters, the pitch of the chiral nematic NCC phase is very sensitive to the ionic strength. By varying the ionic strength, one can control the pitch of the chiral nematic helix and, hence, the colour of the resulting films.[34] An increase in the ionic strength decreases the electrostatic repulsion between NCC particles, which leads to decreasing pitch and finally to a blue shift in the reflected light spectrum of NCC films obtained by the EISA method. However, the colour of the films can be controlled only in particular ranges of pH, ionic strength or precursor concentration, because the liquid-crystalline phase can be lost as a result of, for example, gelation.

The choice of the counter-ion (for the surface sulfo group) has also a considerable influence on the helix pitch, and, hence, colour control can be accomplished by means of appropriate hydroxides for neutralization of NCC suspensions.[54] It was found that an increase in the van der Waals radii of the counter-ions in the series $H^+ < Na^+ < K^+ < Cs^+$ results in increasing helix pitch and in a red shift in the reflected light spectrum of NCC films. The nature of the counter-ion considerably affects the critical concentration for the formation of a chiral nematic phase, the film stability, the temperature dependence of phase separation and repeated dispersibility of the dried films.[34, 36]

In addition, the pitch of the chiral helix is substantially affected by external magnetic fields, drying temperature and ultrasound treatment.[26, 55, 56] Recently, it was found that the contact angle for the substrate on which the NCC films is cast also affects the spectral properties.[57]

The ionic strength, pH of the solution, the nature of counter-ions, temperature variation, pretreatment of the NCC suspension and the substrate material are the tools for controlling the pitch of the chiral helix in NCC films.[57]

Currently, the attempts to control the chiral nematic structure of the films are focused on the use of external impacts: electric or magnetic fields, tangential shear loads and capillary effects.

For example, application of the magnetic field can serve to control the orientation of the cholesteric helix, as the rod-like NCC particles have a negative diamagnetic anisotropy and are located at right angle to the field strength vector.[58–60] Since the rod-like NCC particles are perpendicular to the axis of the cholesteric helix, placing the NCC suspension into a relatively strong magnetic field results in the helix being arranged along the field strength.[61] Using uniform magnetic fields of moderate strength (1 T) and slow evaporation of the solvent, it is possible to obtain films with uniformly oriented cholesteric helices.[62]

The NCC dielectric anisotropy is positive; hence, the external electric field affects the cholesteric structure, by untwisting the helix, *i.e.*, the pitch increases. Habibi *et al.*[63] have shown that NCC particles in the films obtained by drying NCC suspensions can be uniformly aligned by application of electric fields with frequencies ranging from kHz to MHz and amplitude of ~ 2 kV cm^{-1}.

The texture of the NCC films obtained from chiral nematic suspensions is sensitive to shear loads that are applied to the specimen during drying.[64–68] Recent investigations have shown that, for example, nanoparticles of the acidic NCC form (pH 2.0) are arranged at right angle to the shear load, whereas the neutralized form (pH 6.7) is arranged along the load;[65] this provides one of the methods for controlling the pitch of the chiral nematic helix.[69, 70]

It is known that on drying of drops of dilute aqueous suspensions, NCC particles are self-assembled into nematic structures at the edge of dried drops, giving rise to 'coffee-stain rings'.

Figure 23 presents an image of a dried drop of a dilute NCC suspension applied on the specimen glass of the polarized microscope. A red filter (530 nm) gives rise to red colour for the isotropic material and blue and yellow contours for birefringent anisotropic particles. The blue and yellow contours are rather faint, because the initial NCC suspension is dilute and a dried drop forms a very thin film. The blue and yellow rectangles in Fig. 23 show schematically the orientation of rod-like NCC particles tangentially to the edge of the dried drop.

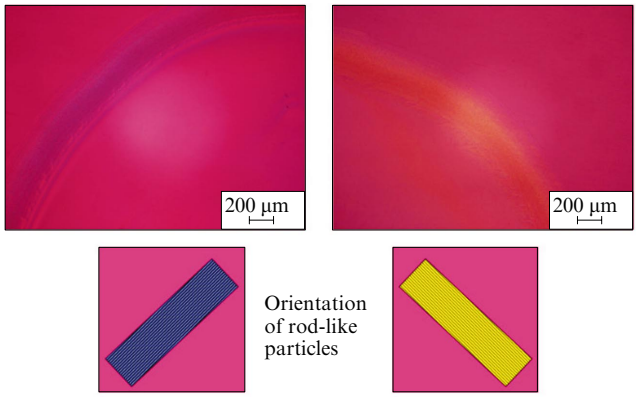


Figure 23. Image of a dried drop of dilute (0.52 mass %) aqueous suspension of NCC obtained by a polarized microscope (crossed polarizers).[28]
Blue and yellow contours observed with a red filter show that anisotropic NCC particles are arranged tangentially to the circle.

Evaporation of concentrated suspensions (above the critical concentration for the formation of the liquid-crystalline phase) induces more substantial structural changes. Preliminary observations of the evaporation of drops of relatively concentrated suspensions show the possibility of formation of drops with 3D iridescent patterns.[71] In that case, the interface at the drop edge was strictly fixed and, as the solvent was evaporated, the NCC particles moved from the centre towards the edge of the drop, demonstrating the 'coffee rings.' An example of the texture of this iridescent film is shown in Fig. 24.

The dark lines in Fig. 24 are the disclination lines at the area borders of mainly planar orientation. The fingerprint lines cannot be seen at this magnification, because the pitch of the chiral nematic helix corresponds to visible wavelengths. The colour of the reflected light

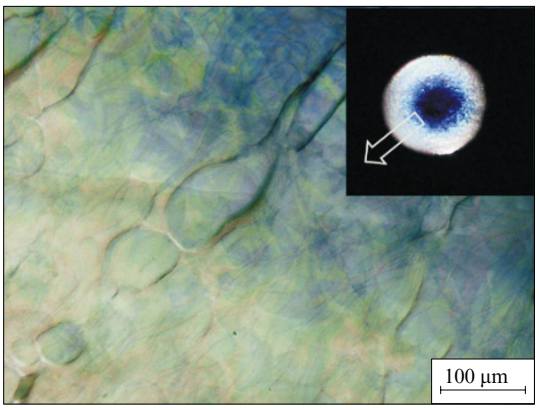


Figure 24. Image of a drop of an aqueous NCC suspension (5.2 mass %) dried on glass.[28]
The image was obtained with a polarized microscope (transmitted image through crossed polarizers). The inset shows the same drop dried on an acrylic surface in the reflected light. The observed iridescent area is marked by an arrow.

changes from blue to red from the centre towards the edge, as shown in the inset of Fig. 24, which reflects the change of thickness across the drop. Similar trends were observed also by Lagerwall *et al.*[24] and Dumanli *et al.*[72,73] Curiously, the colour change from the centre towards the edge is reversed for a drop that has dried between glasses and for NCC films dried in vacuum (that is, the colour changes from red at the centre to blue at the outer edges of the films).[57]

When the interface is not fixed, water evaporation from drops of chiral nematic suspensions is accompanied by a stepwise retreat of the interface from the drop edge towards the centre with gradual increase in the thickness of superimposed layers. In this case, the layers form a complex optical texture (Fig. 25).

The blue band at the very edge shows that nanocrystals are arranged parallel to the film edge. On moving towards the centre of the specimen, there are several separate radially arranged bands with a more complex texture. At higher magnification, it can be seen that these radial bands, each approximately 100–150 μm wide, include wave-like structures, which are ~2 μm wide and up to several hundred micrometres long. These wave-like structures are probably indications of a distorted fingerprint texture.

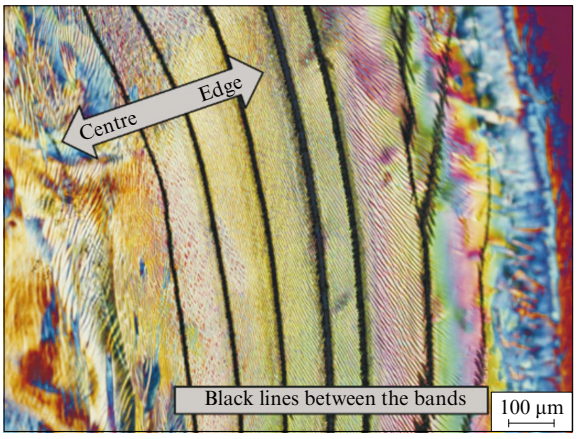


Figure 25. Polarized microscopy image of an NCC film on glass (crossed polarizers, red filter).[28]
The film was prepared by drying an aqueous NCC suspension (6 mass %).

Near the centre, the texture is more uniform, the radial bands are wider and the radial band structure is more clear-cut. In this case, the structures formed are much more sophisticated than the simple planar texture or fingerprint texture obtained for drops with a strictly fixed interface.

Often, it is necessary to suppress the formation of coffee rings, for example, to prepare uniform coatings. In this case, the coffee rings can be reversed by means of the so-called Marangoni effect, which includes surface tension gradient-induced material transfer.[74] For example, the addition of ethanol to a suspension of NCC creates the Maragoni flow, which directs the NCC particles to the centre of the drop and prevents them from concentrating at the edge.[75]

For discussing the coffee rings as applied to NCC, it is necessary to make some remarks and definitions.

In a frequently cited paper of 1997, Deegan *et al.*[76] described the material transfer from the drop centre to the perimeter with the formation of concentric rings — coffee stain rings. The authors attributed this process to the capillary flow that arises upon liquid evaporation and forces the particles dispersed in the liquid to move from the centre towards the edge. The process is universal and does not depend on the substrate nature, the solute or the liquid. However, certain conditions should be met: 1) the contact angle for substrate wetting with the liquid differs from zero; 2) the interface is strictly fixed and does not shift as the drop is dried; 3) the liquid evaporates.

However, the mechanism of formation of coffee rings proposed by Deegan *et al.* referred only to spherical particles.[77] Yunker *et al.*[78–80] have shown that the coffee ring formation depends also on the particle shape and is completely suppressed in the case of anisotropic particles.

Despite the obvious contradiction, in numerous studies devoted to structurization of anisotropic NCC particles at the interface, these phenomena are attributed in some way to the effect of coffee rings. However, it must be admitted that, despite quite a few attempts, no theoretical model describing structurization of anisotropic particles at the interface has yet been developed.[81–83]

Profilometric measurements show considerable deviations from film planarity as a result of capillary effects. By atomic force microscopy, it is possible to observe the orientation of single nanocrystals in solid films. In the films cast from dilute NCC suspensions (below the critical concentration for the formation of the liquid-crystalline phase), the nanocrystal orientation is mainly chaotic, although during the solvent evaporation, the suspension should pass through the concentration range in which the formation of the chiral nematic phase is expected.

The surface orientation of NCC particles in the films cast from concentrated suspensions (above the critical concentration for the formation of the chiral nematic phase) is quite different. Typical atomic force microscopy

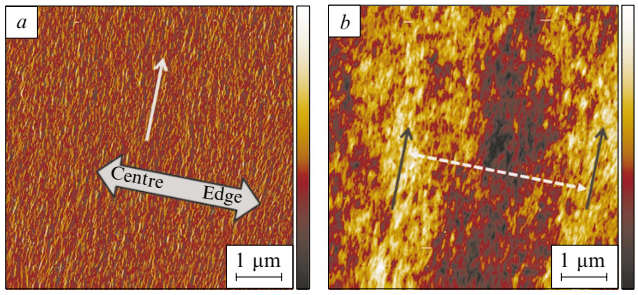


Figure 26. Atomic force microscopy image of the surface of a film cast from an aqueous NCC suspension (8 mass %) on mica.[28] (*a*) Amplitude image (white arrow shows the approximate orientation of nanocrystals); (*b*) profile image (black arrows show the arrangement of combs; the colour scale of the profile is from −19 to +19 nm).

images of the surface of a film (cast on mica from a 8% suspension of NCC) are shown in Fig. 26.

In the amplitude image (see Fig. 26 *a*), it can be seen that NCC particles are evenly oriented parallel to the edge of the specimen. The profile image shows (see Fig. 26 *b*) that the surface is rough and has combs with up to 10 nm height, also oriented parallel to the edge and separated by 2 – 3 μm distances. The distance between the combs observed by atomic force microscopy is of the same order of magnitude as the distances between the lines in the fingerprint textures, which are detected by optical microscopy. It is reasonable to assume that these combs arise as a result of anisotropic orientation of NCC particles in the film.

The possible explanation is presented in Fig. 27. The orientation of the neighbouring layers of anisotropic particles of the chiral nematic structure near the film surface is shown in Fig. 27 *a*. The axis of the cholesteric structure is perpendicular to the plane of the drawing (parallel to the specimen surface) and we observe particular segments of the chiral helix, which screen one another and penetrate into the bulk at right angle to the plane of the drawing. Successive movement from left to right gives an idea of particle orientation in space with a period of $P/2$ (see Fig. 27 *a*). If we assume that film shrinkage during drying is not uniform, in particular, it is most pronounced across the particle and less pronounced along the particle, as shown in Fig. 27 *b*, the appearance of combs shown in Fig. 26 can be understood. The distance between the combs is half the pitch of the chiral nematic structure ($P/2$).

It is obvious that the presented model is much simplified. Shrinkage during drying does not necessarily occur perpendicularly to the specimen plane and the chiral nematic axis may be arranged at an angle to the surface. Nevertheless, one can expect that studying the surface topology by means of atomic force microscopy would supplement and extend the potential of polarized optical microscopy.

While studying the appearance of coffee rings upon the formation of NCC films, Uetani and Yano[84,85] observed that the NCC particles are arranged parallel to the film edge, whereas the particles at the centre are arranged chaotically (Fig. 28).

Mashkour *et al.*[86] studied the self-assembly of NCC particles and poly(vinyl alcohol) on planar inclined and

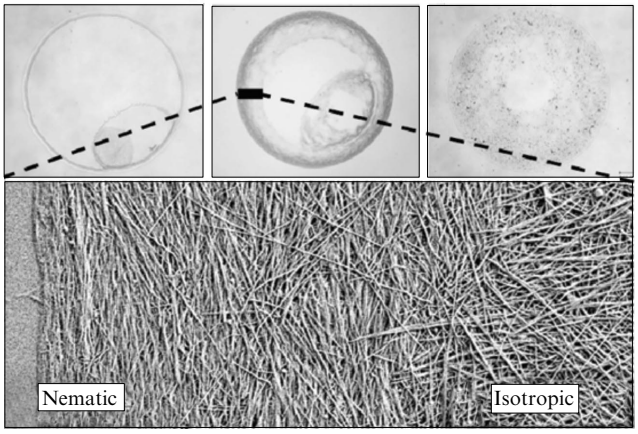


Figure 28. Orientation of rod-like NCC particles at the edge of the coffee ring (field emission scanning electron micrograph).[84]

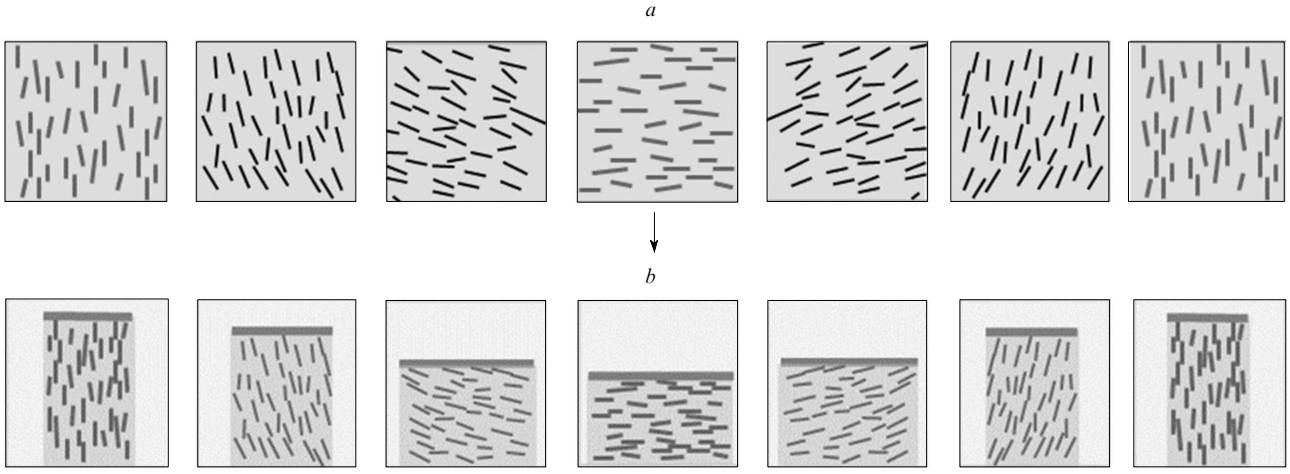


Figure 27. Presumptive mechanism of the appearance of surface combs with $P/2$ period (see the text).[28]

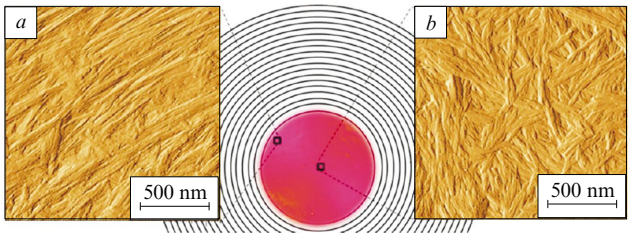


Figure 29. AFM micrograph of a film obtained by evaporation of an aqueous suspension of NCC in a concave glass vessel.[86]
It can be seen that NCC particles are located tangentially to the surface at the film edge (*a*) and chaotically at the film centre (*b*).

curved surfaces and drew some interesting conclusions. They found that if the substrate on which the NCC suspension is evaporated is somewhat inclined, this gives rise to an additional driving force, which promotes the arrangement of rod-like NCC particles parallel to the dry-line boundary. If the NCC suspension is placed into a concave glass mould that is sufficiently narrow to have a noticeable meniscus, this also affects the morphology of the forming film (Fig. 29).

The tangential alignment of rod-like NCC particles occurs at the interface between the liquid and the substrate surface. The arrangement of particles is controlled, first of all, by the Brownian motion and surface tension. It is noteworthy that the behaviour of NCC controls the self-assembly of the polymer chains of poly(vinyl alcohol).[86, 87]

Thus, a study of just evaporation of aqueous suspensions of NCC reveals a series of self-assembly phenomena.[28]

1. In NCC suspensions with concentrations either much lower or much higher than the critical concentration for the formation of the liquid-crystalline phase, NCC particles tend to align tangentially at the edge of the drop.

2. Dried drops of concentrated NCC suspensions have a surface microrelief determined by mass transfer from the centre to the periphery during solvent evaporation (so-called coffee-stain ring effect).

3. The coffee-stain ring effect is most pronounced for drops with the fixed interface; in this case the dried film thickness is several times greater at the edge than at the centre.

4. When the interface is weakly fixed, it moves stepwise towards the centre of the drop with a gradual increase in the thickness of the superimposed layers. The layers form a sophisticated optical texture.

5. The surface microrelief of the dried films studied by atomic force microscopy displays combs of about 10 nm height located at a distance of a half chiral helix pitch ($P/2$). The appearance of the combs is attributable to the anisotropic shrinkage of the chiral nematic films during solvent evaporation.

The multicolour chiral nematic films were obtained by Dumanli *et al.*[72] by slow evaporation of NCC suspensions in polystyrene Petri dishes. According to polarized optical microscopy data, the films selectively reflect left-hand circularly polarized light in a definite wavelength range. The film colour is due to the presence of differently coloured separate domains with sizes from several micrometres to several tens of micrometres. Scanning electron microscopy confirms that the domains have a left-handed helical structure and consist of multilayers with a definite pitch of the cholesteric helix. In domains of the same colour, the helix pitch is strictly defined. The domains are separated by defects, which are formed at the sites in which the axis of the chiral nematic helix changes its orientation. The authors showed that the self-assembly and formation of the multidomain structural colour largely depend on the polydispersity of NCC particles.

The images obtained by a polarized optical microscope demonstrate a mosaic pattern composed of domains of various shapes and sizes and of three major colours: green, blue and orange (Fig. 30 *a*). In order to elucidate the origin of the colours, the film cross-sections were studied by SEM (Fig. 30 *b–d*). The layered left-handed helical structure can be clearly seen in the SEM images; the uniformity of the cholesteric structure is well preserved along the film fracture surface.

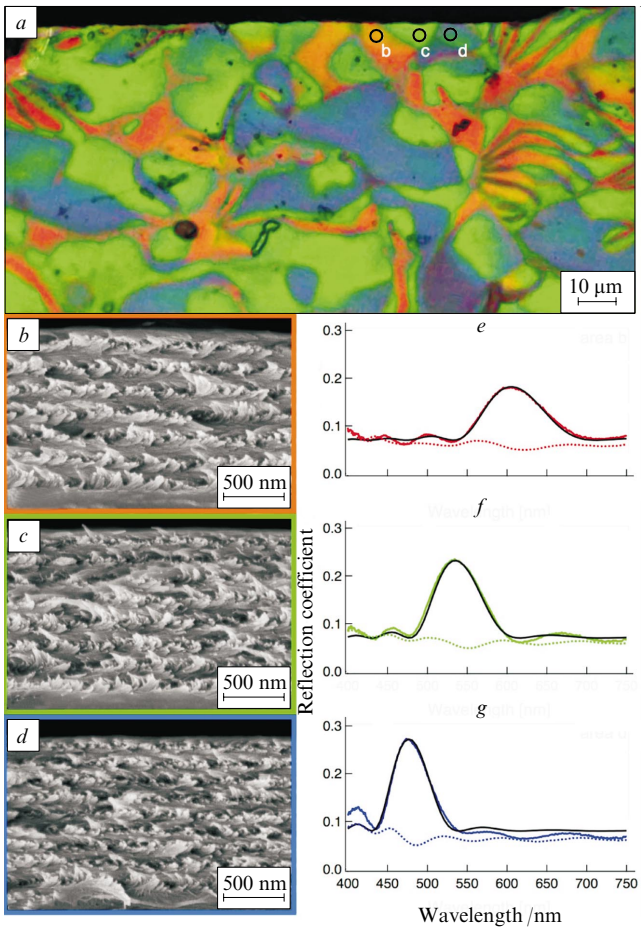


Figure 30. Comparison of the results of studies of multicolour NCC films by optical and electron microscopy.
(*a*) Polarized optical microscopy image (left-hand circular polarization) of the NCC film. Black circles show areas **b**, **c** and **d**, corresponding to the SEM images (cross-section) (*b–d*) and reflection spectra (*e–g*).[72] The black continuous lines in the spectra show the Berreman matrix approximation of the spectral curves.[88, 89]

Table 1. Reflection peak wavelength (λ) and pitch of the chiral nematic helices of various domains in NCC film (see Fig. 30).[72]

	Domain **b**	Domain **c**	Domain **d**
Domain colour	Orange	Green	Blue
λ (nm), found from the spectrum	590	530	470
P (nm), found by SEM	190 ± 15	170 ± 10	150 ± 10
λ (nm), calculated from P	593	530	468

The relationship between the reflected light wavelength and the helix pitch of the chiral nematic structure is expressed by Eqn (2). If the light reflection angle is assumed to be close to 90°, the reflected light wavelength is determined by the helix pitch: the greater the P value, the higher λ.

The pitches of the chiral nematic helix measured by SEM (areas **b**, **c** and **d** in Fig. 30 *a*) were compared with the reflection peak wavelengths (see Fig. 30 *e*,*f*,*g*). The results are presented in Table 1.

It can be seen from Table 1 that the reflection peak wavelengths derived from spectral data and calculated using the pitch of the chiral nematic helix are in excellent agreement with each other.

Analysis of POM and SEM images showed that within the domains with different structural colours, the chiral nematic structure is fairly uniform. Furthermore, the chiral nematic order is preserved over distances of up to several tens of micrometres, which is 10 – 100 times as great as the length of single nanocrystals. Nevertheless, defects can be clearly seen at the domain boundaries; one of these defects is seen in Fig. 31.

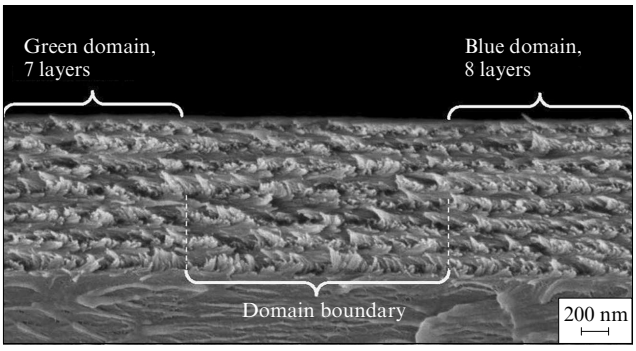


Figure 31. SEM image of the transition boundary between two domains with different structural colours — green and blue.[72]

The transition between the domains with different pitches of the cholesteric helix is clearly seen in Fig. 31: the green domain composed of 7 layers is separated from the blue domain composed of 8 layers by the disclination region. The authors concluded that a necessary condition for attaining a uniform colour of the film of a specified thickness is the monodispersity of NCC particles, which would allow one to strictly control the pitch of the chiral nematic helix.

V. Functional materials obtained by nanocrystalline cellulose-templated sol – gel synthesis

Functional nanostructured materials can be obtained by various methods such as layer-by-layer sputtering, centrifugation, Langmuir – Blodgett process, *etc*. However, considering the simplicity and efficiency, EISA is the method of choice for preparing functional materials by NCC-based templated synthesis. This approach includes mixing of an NCC suspension with a compatible precursor (compound participating in the reaction to be converted to the target product) for the formation of a nanostructured composite material. The subsequent selective removal of the template from the composite gives a porous material representing a mesoporous negative solid duplicate of the liquid-crystalline mesophase.

The most notable feature of the described materials is their nanostructure, which is responsible for the structural colour resulting from selective reflection of the circularly polarized light. In Nature, the structural colour plays an important role in signal transduction, mimicry and selection of the partner for reproduction.[51] The bright colour of quite a number of mussels, the insect armour and bird feathers arises as a consequence of 3D hierarchical structure of biomolecules. These natural, so-called photonic, structures inspire researchers to design novel materials with structure-controlled spectral properties to be used in sensorics and optoelectronics. An effective approach to the development of photonic materials is the use of templates ordered *via* molecular assembly. The subsequent removal of the template gives rise to ordered structures with controlled spectral properties. The structure periodicity can be changed by varying reaction conditions; this provides control over the properties of the resulting materials. Depending on the function and practical application, the structural colour of the material can be tuned by changing either the refractive index or the helix pitch of the chiral nematic structure.

For successful duplication of the structural features of the liquid-crystalline template in a composite material, several conditions should be met.[20] First, the precursor should be compatible with the template and the solvent, *i.e*., they must be miscible. The template concentration, pH and ionic strength of the medium are crucial for the compatibility, because extreme pH values or the presence of the precursor may induce gelation and destruction of the liquid-crystalline phase. Second, the kinetic parameters of the condensation (or polymerization) reaction, which results in the formation of the composite material, should allow the template to form an ordered liquid-crystalline phase before the matrix is completely cured. Third, all side products of the condensation (polymerization) reaction should be easily evaporated or be compatible with the liquid-crystalline phase of the template. If these conditions are met, a liquid-crystalline phase is formed and its structure is preserved in the nanocomposite upon solvent removal and curing. During the template synthesis, the structural features of the liquid-crystalline phase are retained in the composite material, and the subsequent template removal affords porous materials with a large specific surface area.

Although chiral composite films can themselves act as functional materials,[90, 91] the presence of developed porosity and large specific surface area markedly extend the scope of potential applications of chiral nematic materials. Selective removal of one component of the composite may be problematic; therefore, for each composite material, it is necessary to thoroughly select conditions suitable for selective removal of one component, with the other component remaining intact. Furthermore, it is very important to observe conditions that would prevent the collapse of the porous structure after removal of the template.

Calcination in air is the most common and simplest process for removing organic templates from composites with an inorganic matrix. Nanocrystalline cellulose-based templates are usually removed by calcination in air at temperatures >250 °C. If milder conditions are needed, acid or base hydrolysis of cellulose is used.

The template removal has a considerable influence on the structure and photonic properties of the resulting mesoporous samples. The removal of NCC template (refractive index $n = 1.51$)[20] gives rise to air-filled pores ($n = 1.00$), which decreases the average refractive index of the mesoporous material and induces a blue shift in the reflected light spectrum. Calcination may induce film shrinkage, which decreases the average pore size and also induces a decrease in the reflected light wavelength. As a rule, the pitch of the cholesteric helix of the composite before calcination is greater than the visible light wavelength; therefore, the initial composite films are uncoloured. After removal of the NCC template, the resulting mesoporous film often exhibits the Bragg reflection in the visible spectral range and characteristic iridescent colour in the polarized light. Scanning electron microscopy data show in this case that NCC removal decreases the pitch of the cholesteric helix down to several hundreds of nanometres (the allowed photonic band corresponds to visible wavelengths), *i.e.*, the films acquire a structural colour visible by the naked eye.

For manufacturing materials that cannot be obtained by conventional template synthesis, *e.g.*, because of instability of the precursor, so-called hard templating (nanocasting) with a pre-formed mesoporous matrix is used.

Figure 32 shows the chart of various synthetic strategies used to produce nanostructured materials using NCC as the template.

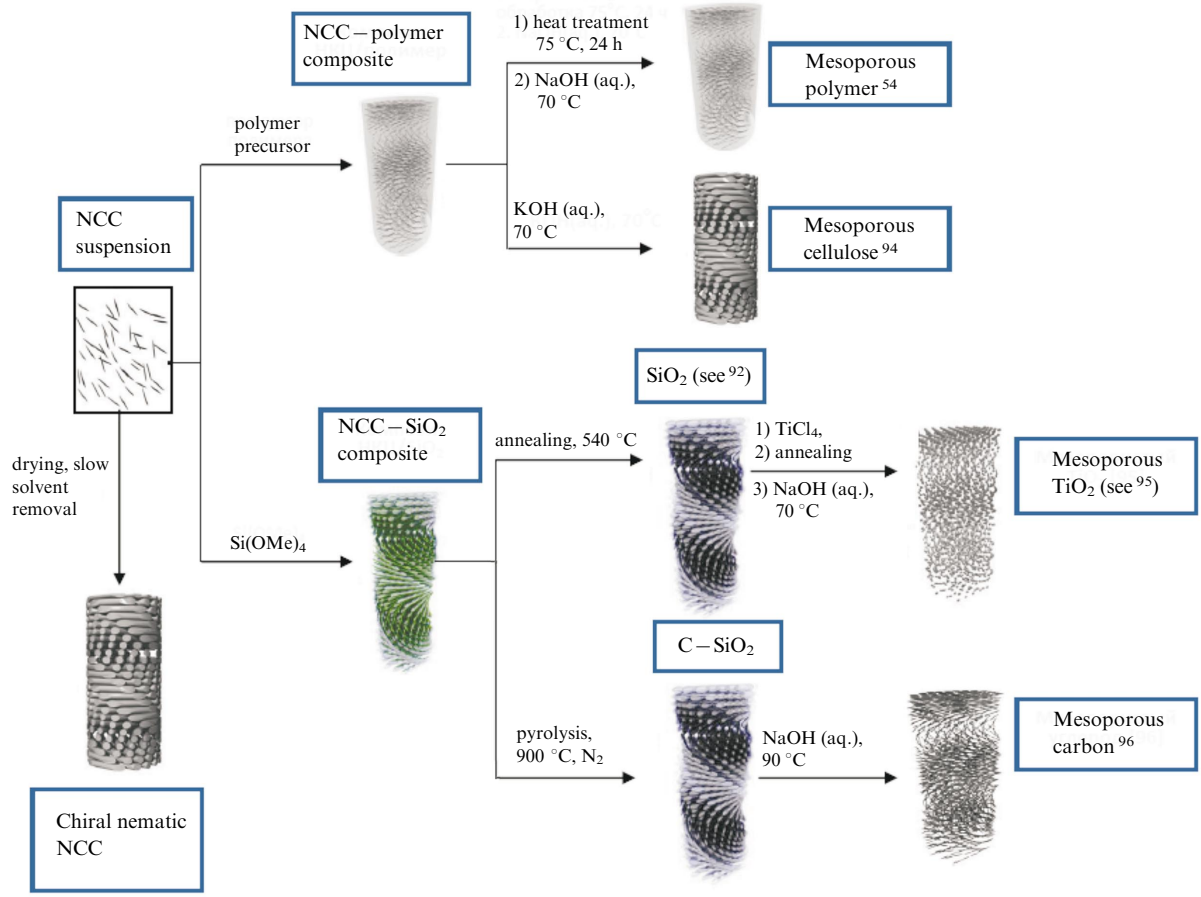


Figure 32. Schematic chart of the synthesis of nanostructured materials with NCC as the template.
In the presence of an appropriate precursor, NCC forms a composite with a chiral nematic structure. Removal of the NCC template affords a mesoporous material, which can be functionalized by surface modification or impregnation of pores or used as the template in the subsequent synthesis (hard templating, the upper right picture). An alternative removal of the inorganic matrix after NCC carbonization leads to the formation of chiral mesoporous carbon. The chart is based on a number of publications.[20, 51, 91–99]

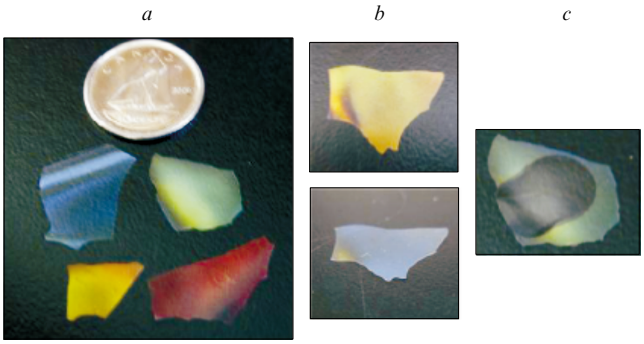


Figure 33. Photographs showing different colour of mesoporous silica films.[92]
(*a*) The structural colour of films is due exclusively to the formation of the chiral nematic porous material structure and depends on the pitch of the chiral helix (for evaluation of the specimen size, a coin 18 mm in diameter is shown); (*b*) the specimen colour changes for different viewing angles; (*c*) the specimen loses colour and becomes transparent upon wetting with water.

In 2010, MacLachlan and co-workers[92] found for the first time that alkoxysilane precursors such as tetramethoxysilane (TMOS) or tetraethoxysilane (TEOS) are compatible with aqueous NCC suspensions and that EISA affords uniform bright iridescent-coloured composite films. The reflected light spectra for the specimens varied over a broad range from UV to near-IR region, depending on the silica : NCC ratio and the salt added.[93] The intense positive circular dichroism signal corresponding to the absorption maximum in the UV/Vis spectrum pointed to the predominant reflection of the left-hand circularly polarized light, thus indicating the formation of a left-handed chiral structure. The composite self-assembly was found to occur in a narrow pH range of the suspension (approximately from 2.4 to 4); beyond this range, optically non-transparent achiral films were formed. Since the refractive indices of NCC and silica are close, the shift of the reflection spectrum is mainly dictated by the change in the chiral helix pitch. The removal of cellulose by calcination yielded mesoporous silica films with iridescent colour characteristic of a chiral nematic structure (Fig. 33). Transmission electron microscopy images and low-temperature nitrogen adsorption measurements prove a large surface area of the calcined silica films (300 to 800 $m^2\ g^{-1}$) and existence of mesopores with the volume ranging from 0.25 to 0.60 $cm^3\ g^{-1}$, depending on the composition of the initial composite. The pore size distribution determined by the Barrett – Joyner – Halenda method has a maximum at pore diameters of 3.5 to 4.0 nm; this implies successful imprinting of single NCC particles (unlike the aggregates) in the porous silica structure. This pore size is smaller than the diameter of single NCC particles. Probably, silica pore walls are contracted during calcination, which results in a blue shift in the reflected light spectrum with respect to that of the composite film. The bright iridescent colour and birefringence clearly observed for the calcined films through a polarized microscope are caused by anisotropy of the mesoscopic pore ordering induced by self-assembly of NCC particles.

The introduction of organic functional groups into mesoporous silicas provides the opportunity for further improvement of their properties. A large success along this line is associated with the discovery of the possible use of precursors such as $(RO)_3Si-R'-Si(OR)_3$ (R' is an aliphatic or aromatic group) in the sol – gel synthesis of mesoporous organosilicon structures.[100] The direct use of such organosilicon precursors has obvious advantages over the introduction of functional groups after the synthesis, as it provides strict stoichiometric control over the relative contents of inorganic and organic components in the hybrid material. The introduction of cross-linking organic functional groups as structure constituents not only changes the chemical environment inside the pores, but can also modify the material properties such as molecular structure, mechanical strength, hydrothermal stability and so on. To prevent the thermal destruction of organic cross-links during the preparation of organosilicon materials, a special procedure has been developed for removing NCC templates. Treatment with 6 M sulfuric acid at 100 °C for 18 h selectively removes NCC, without affecting the chiral nematic structure of the organosilicon matrix. The subsequent washing with dilute aqueous H_2SO_4 removes the remaining cellulose decomposition products and gives transparent and completely colourless films, which become iridescent after drying. Alternatively, hydrochloric acid treatment followed by washing with hydrogen peroxide is used. Complete removal of NCC and retention of organosilicon compounds in pore walls was confirmed by solid-state ^{13}C and ^{29}Si NMR spectroscopy. As compared with brittle silica films prepared from TMOS and TEOS precursors, the organosilicon films show markedly enhanced mechanical properties, flexibility and ultimate strength.

Shopsowitz *et al.*[96] developed a simple method for the synthesis of mesoporous carbon with a large specific surface area, a large pore volume and a chiral nematic structure. According to this method, NCC – silica composite films are first produced, as described above for the synthesis of mesoporous chiral silicon dioxide films. Pyrolysis of the NCC – silica composite at 900 °C in a nitrogen atmosphere gives the carbon – silica composite. Thermogravimetric (TG) analysis shows that decomposition of NCC yields up to 30 mass % mesoporous carbon. The mesoporous carbon films were obtained by selective etching of the carbon – silica composite with an aqueous solution of alkali.

The obtained material is a glossy black film containing 90% of carbon, according to elemental analysis data (Fig. 34 *a*). Powder X-ray diffraction and Raman spectroscopy confirmed that NCC pyrolysis in an inert gas atmosphere gives rise to amorphous carbon. The porosity of carbon films depends on the content of silica in the composite. Carbon films obtained directly from NCC possessed mainly microporosity, whereas NCC – silica composites with NCC content of 65 mass % were fully mesoporous. The pore surface area and volume for the mesoporous carbon were 570 – 1460 $m^2\ g^{-1}$ and 0.3 – 1.2 $cm^3\ g^{-1}$, respectively, depending on the material composition. The SEM analysis of these specimens showed a twisted morphology similar to that of the corresponding silica samples, which is indicative of the left-handed chiral nematic structure of the resulting

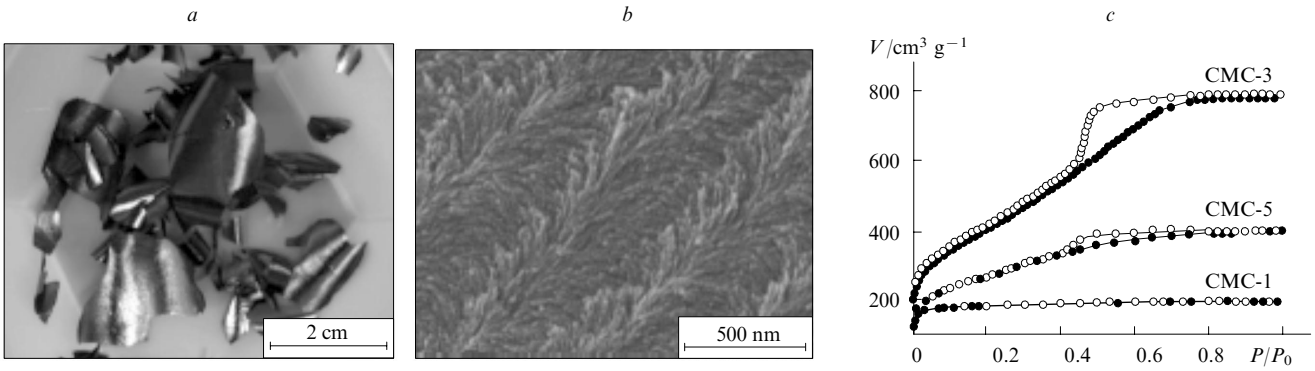


Figure 34. Photograph of mesoporous carbon films of the CMC-3 specimen (*a*), SEM image of the fracture cross-section of the CMC-3 film (*b*), nitrogen adsorption isotherms on mesoporous carbon specimens (*c*).[96]
Mesoporous carbon specimens were obtained from NCC (CMC-1) and NCC–SiO_2 composites containing 65 mass % (CMC-3) and 43 mass % NCC (CMC-5).

mesoporous carbon films (Fig. 34 *b*). An important application of porous carbon materials is the manufacture of electronic devices. Mesoporous carbon behaves as a semiconductor; recently, it was shown that the semiconductor mesoporous carbon is an efficient material for the design of field effect transistors; it can be used in gas sensing devices and is a promising material for electrodes of supercapacitors.[96, 101]

Hard templating can be used to prepare stable mesoporous TiO_2 films with a great specific surface area (150–230 m^2 g^{-1}), preserving a chiral nematic structure.[95, 97] For this purpose, NCC is removed from the NCC–silica composite by calcination at 540 °C or by treatment with strong acids to give chiral nematic silica films. After that, the silica films are treated with an aqueous solution of $TiCl_4$, dried and annealed at 200 °C and then calcined at 600 °C to give a crystalline product, which is treated with 2 M aqueous NaOH. This gave mesoporous TiO_2 films with a left-handed chiral nematic structure (Fig. 35). These highly porous TiO_2 films can be used in dye-sensitized solar cells, in photocatalysis and in sensing devices.

Recently Chu *et al.*[102] used an analogous hard templating approach to obtain chiral nematic zirconium dioxide (ZrO_2) films and also europium-doped zirconium dioxide (ZrO_2/Eu^{3+}) films. The ZrO_2/Eu^{3+} films exhibit luminescence characteristic of Eu^{3+} in combination with photonic properties generated by the chiral nematic structure.

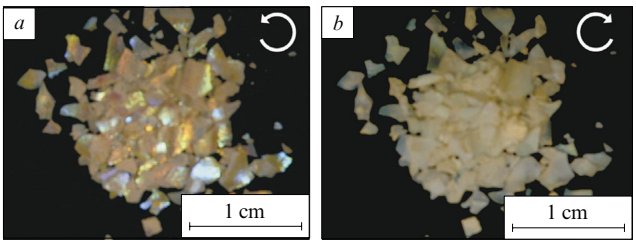


Figure 35. Photographs of mesoporous TiO_2 films in left-hand (*a*) and right-hand circularly polarized light (*b*).[95]

Mehr *et al.*[98] described polymerization of the conjugated poly(*p*-phenylenevinylene) polymer in the pores of the chiral nematic mesoporous organosilicon structure, giving rise to composite films possessing a structural colour and exhibiting a strong characteristic fluorescence of the polymer.

Thorough investigation of the circular dichroism shows the presence of a chiral polymer structure inside the pores. It was found that in this composite material, fluorescence quenching takes place upon interaction with electron-withdrawing organic compounds, for example, 2,4,6-trinitrotoluene, which may imply the possible use of this material for the design of chemical sensors. Poly(*p*-phenylenevinylene) attracts enhanced attention of researchers for its potential uses in a number of fields such as electronics, chemosensorics and so on. Unfortunately, application of devices based on poly(*p*-phenylenevinylene) under ambient conditions leads to gradual degradation of the polymer as a result of interaction with atmospheric moisture and oxygen. An efficient method for preventing the degradation is to encapsulate poly(*p*-phenylenevinylene) into porous materials, which are readily accessible by self-assembly in solution.

Qi *et al.*[103] and Kelly *et al.*[104] reported the successful synthesis of mesoporous silica with metal nanoparticles encapsulated in the pores. The nanoparticles of noble metals (silver, gold, platinum) encapsulated in the pores of chiral nematic silica exhibit strong circular dichroism associated with the surface plasmon resonance, which arises due to the helical arrangement of metal nanoparticles. Currently, the surface plasmon resonance phenomenon is widely used in the design of chemical and biological sensors. On contact with biological specimens (DNA, viruses, antibodies), plasmon effects can enhance fluorescence intensity by more than an order of magnitude; in other words, they substantially increase the possibilities of detection, identification and diagnosis of biological specimens.

One more field of growing interest in functional materials is the preparation of hybrid materials with quantum dots.[105] Combination of the optical properties of photonic crystals with the electronic characteristics of semiconductor quantum dots may give rise to novel functional materials that could find use in optoelec-

tronics, sensorics, optical amplifiers and lasers. In 2014, Nguyen *et al.*[105] published the first paper about a hybrid material obtained by NCC-templated sol–gel synthesis and combining the iridescent colour of chiral nematic silica with CdS luminescence.

Apart from the above inorganic composites, numerous polymeric NCC composites have been reported. The first publications along this line are related to NCC used as a filler for improving the mechanical properties of composites.[106] In the case of materials comprising two organic compounds with similar characteristics (NCC and polymer), selective removal of one of them is a challenge. However, removal of the NCC template from the polymer matrix gives rise to a mesoporous structure, which extends the scope of potential applicability of this material. MacLachlan and co-workers [51, 90, 94] published a series of papers describing mesoporous films of phenol formaldehyde and melamine urea formaldehyde resins, which possess a chiral nematic order inducing structural colouring.

Mixing of aqueous suspensions of NCC (3 mass % – 5 mass %, pH 2.4–6.9) with precursors based on water-soluble formaldehyde resins yielded stable composite films, which possessed a chiral nematic structure after drying under ambient conditions (Fig. 36).[51] The NCC template was selectively removed by treating with a 16% aqueous solution of NaOH at 70 °C for 8–12 h. This treatment afforded a mesoporous chiral nematic resin and resulted in the removal of 85%–90% of NCC from the polymer matrix, as shown by IR spectroscopy, solid-state NMR spectroscopy and TG analysis.

Giese *et al.*[94] selectively removed the polymer from the NCC–polymer (urea formaldehyde resin) composite films to give mesoporous photonic cellulose. These films exhibited excellent wettability because of their mesoporous structure; in addition, they changed their colour within several seconds, depending on the wetting liquid (water or ethanol). The colour of the films gradually changed with changing content of ethanol in water; the colour change can be easily detected by means of UV/Vis or CD spectroscopy and can also be seen by the naked eye (Fig. 37). High flexibility of specimens and fast response to a change in the solvent polarity makes them

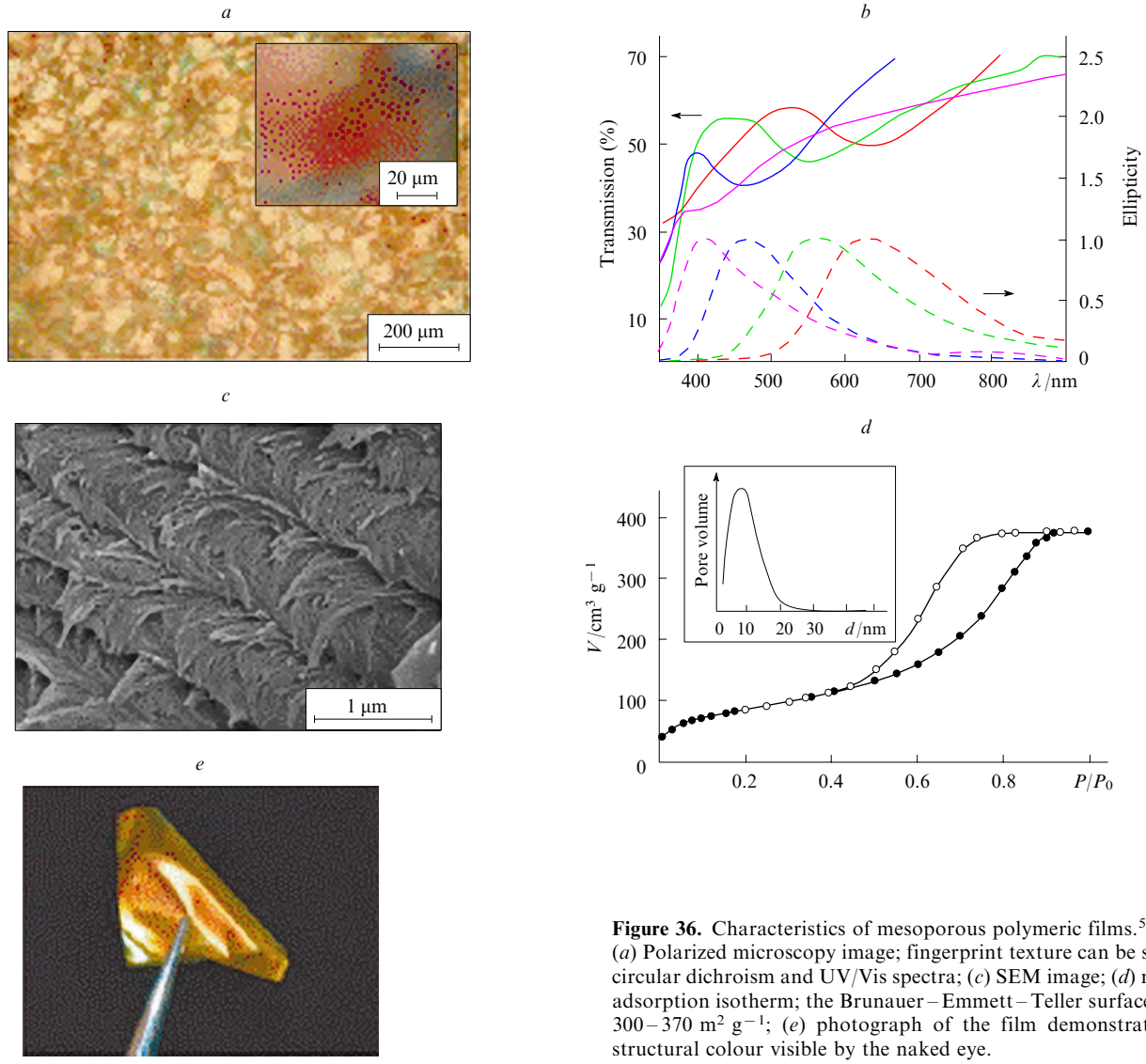


Figure 36. Characteristics of mesoporous polymeric films.[51] (*a*) Polarized microscopy image; fingerprint texture can be seen; (*b*) circular dichroism and UV/Vis spectra; (*c*) SEM image; (*d*) nitrogen adsorption isotherm; the Brunauer–Emmett–Teller surface area is 300–370 $m^2\ g^{-1}$; (*e*) photograph of the film demonstrating the structural colour visible by the naked eye.

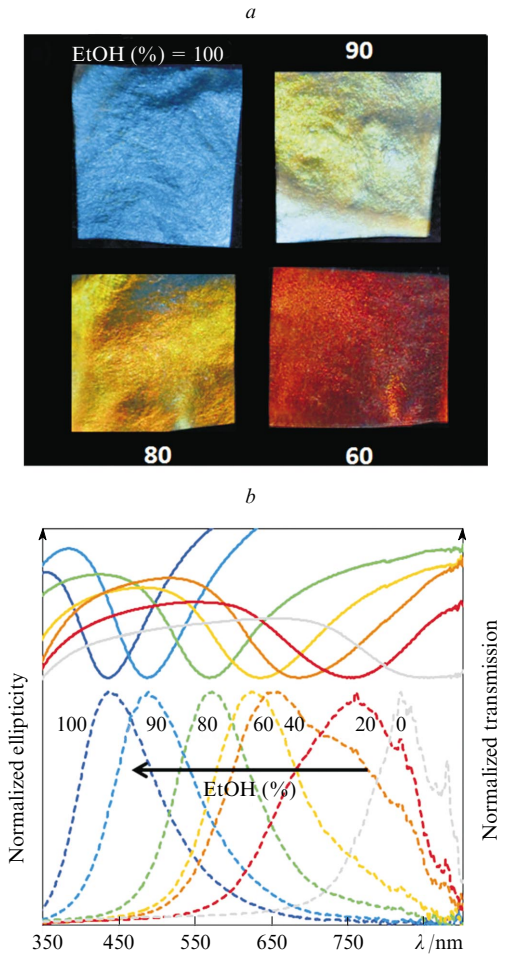


Figure 37. Structural colour of mesoporous photonic cellulose films *vs.* wetting liquid composition: the colour varies from blue in pure ethanol to red in aqueous ethanol with ethanol content of 60% (*a*).[105]
UV/Vis and CD spectra (continuous and dashed lines, respectively) of films wetted with EtOH – H_2O mixtures of various composition (ethanol content in the mixture is indicated in the Figure). It can be seen that with increasing ethanol content, the peaks shift to shorter wavelengths.

very attractive for potential applications in optics and sensorics.

The development of flexible photonic materials capable of multi-colour reflections extends the scope of their practical use in displays, sensors and optoelectronics. Furthermore, the application in technology can be extended by combining the controllable photonic properties of the synthesized materials with the mechanical properties permitting a response to external stimuli. The synthetic materials able to mimic the natural contractile motion (muscle activity; microorganism-like motion) attract huge interest because of their possible application in various actuation systems, microfluidic elements and microrobotics. The polymers capable of responding to an external stimulus are excellent candidates for these types of application owing to low density, elasticity, low cost and easy preparation.

Khan *et al.*[99] demonstrated that a two-layer phenol formaldehyde resin film can be fabricated by simple successive deposition of the layers. An aqueous NCC dispersion was mixed with a solution of the resin precursor in aqueous ethanol. The resulting homogeneous suspension was poured out into Petri dishes; drying under ambient conditions yielded an intensely coloured composite film. The second layer was formed by casting of an aqueous dispersion of the NCC – precursor mixture of a different composition onto the first layer. Complete drying of the suspension gave brightly coloured iridescent two-layer composite films. The films were cured with heating and treated with an aqueous solution of NaOH to remove NCC. Drying in supercritical CO_2 gave mesoporous, elastic two-layer phenol formaldehyde films with a chiral nematic structure, which possessed a unique combination of controlled optical properties and fast mechanical response (Fig. 38).

The two layers of the film differed in the pitch of the chiral helix and, as a consequence, they selectively reflected light at two different wavelengths and underwent the expansion or compression to different extents under the action of a solvent. The structural differences of two layers determine the colour change and their ability to curl or uncurl on drying and wetting correspondingly. The mesoporous structure of the two-layer films makes the response to the external stimulus very fast.

In 2013, Kelly *et al.*[91] described nanocomposite hydrogels with chiral nematic structure and interesting photonic properties. Hydrogels can be easily prepared by self-assembly of aqueous NCC dispersions with various monomers including acrylamide, *N*-isopropylacrylamide, acrylic acid, 2-hydroxyethyl methacrylate, poly(ethylene glycol dimethacrylate) and poly(ethylene glycol methacrylate) in the presence of a photoinitiator and a cross-linking agent followed by UV-initiated polymerization. The properties of hydrogels vary over wide ranges depending on the chosen monomer. NCC-based hydrogels show colour changes in response to a change in the external stimulus, such as temperature, pH, solvent polarity; that is, they possess controlled functionality. According to predictions, these hydrogels would find use as sensors or controlled light filters and for soft templating to obtain new materials.

Until recently, the formation of chiral nematic order was studied only in aqueous suspensions of NCC, which considerably restricted the choice of suitable precursors, because many of them are unstable or insoluble in water, or the condensation involving them is too fast and prevents the self-assembly to a chiral structure. The dispersibility of NCC in organic solvents can be markedly increased, for example, by surface modification of NCC or by surfactant adsorption. In some cases, dispersions of modified NCC actually form chiral nematic phases in organic medium, but the chiral structure is not retained in dried films.

Cheung *et al.*[54] reported that neutralization of the acidic NCC form (H-NCC) by strong bases (alkali metal or quaternary ammonium hydroxides) followed by freeze drying affords the neutralized NCC form (X-NCC, $X = Li^+$, Na^+, K^+, NH_4^+, Me_4N^+, $Bu^n_4N^+$), which is easily dispersed in polar aprotic organic solvents such as DMSO, formamide, *N*-methylformamide and dimethylformamide. Dispersions of X-NCC in polar organic solvents form chiral nematic phases *via* EISA, which gives rise to solid films with chiral photonic properties,

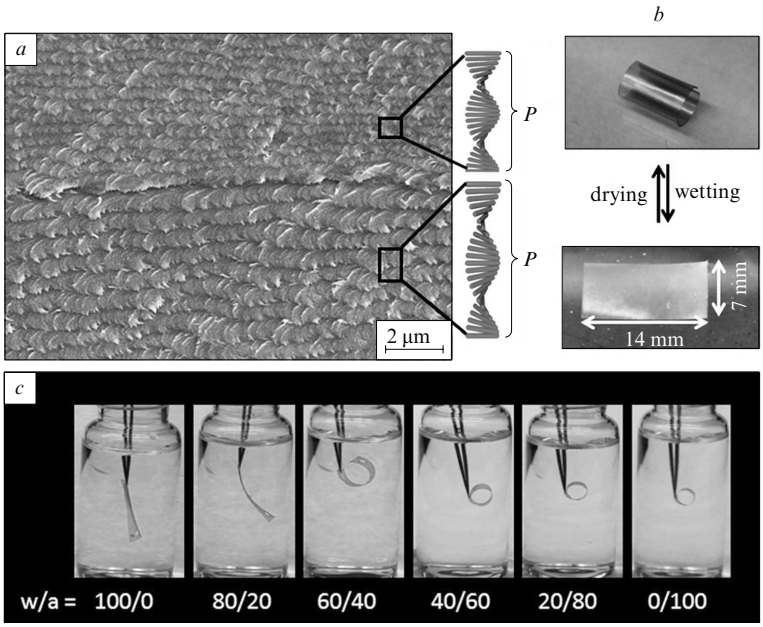


Figure 38. The SEM image of the cross-section of a two-layer polymeric film shows different pitches of the chiral helix in each layer (*a*); photographs of the stretched and rolled two-layer polymeric film, respectively, after wetting with water and drying (*b*); the photographs of the two-layer polymeric film in water – acetone (w/a) mixtures show that with increasing acetone content, the uncurled film completely curls (*c*).[99]

which depend on the initial concentration of X-NCC and the cation size and hydrophobicity. An increase in the cation size induces blue shift in the reflected light spectrum, whereas the red shift occurs with increasing hydrophobicity of alkylammonium cations, which is consistent with the results obtained for aqueous dispersions of X-NCC. The authors demonstrated successful formation of the photonic polymeric composite films upon mixing X-NCC dispersions in DMF with DMF-soluble polymers [polystyrene, poly(methyl methacrylate), polycarbonate and poly(9-vinylcarbazole)].

VI. Conclusion

Nanocrystalline cellulose, which has been known for more than 50 years, attracts considerable attention of researchers for its physical and chemical properties such as the lack of toxicity and biocompatibility, biodegradability, large specific surface area, high elastic modulus and optical characteristics. However, the potential of NCC as a supramolecular template has been discovered not long ago. The discovery of the self-assembly of NCC in aqueous suspensions to give liquid-crystalline structures and then the fabrication of chiral nematic NCC films were the scientific results that predetermined the development of a broad range of structural and functional materials, which are obtained by NCC-based templated synthesis. The unique combination of the chiral nematic structure, mesoporosity and optical characteristics of these materials account for their applications in the design of new functional materials: mesoporous sorbents, photonic crystals, supercapacitors, materials for transistors, sensors and detectors, and for microelectronic and electrooptical devices.

Cellulose, which is readily available and relatively inexpensive, is an environmentally benign, renewable raw material for the production of NCC, thus promoting commercialization of NCC on an industrial scale. In turn, NCC is an excellent liquid-crystalline template for the synthesis of a broad range of mesoporous materials with useful functional properties. The liquid-crystalline properties of NCC suspensions and compatibility of NCC with many inorganic and polymeric precursors ensures the optimal course of synthesis to form functional materials. The chiral nematic liquid-crystalline structure of NCC suspensions is retained in the films after removal of the template, thus giving rise to the porous chiral structure and initiating the controlled photonic properties. Functionalization of the porous structure additionally extends the scope of applicability of the new materials. These materials open up wide opportunities for scientific research and practical application. With technical refinement, NCC-based materials would be commercialized and would find use as optical filters, polarizers, electrode materials, capacitors and so on.

One issue hampering commercialization of NCC-based materials is a rather costly NCC isolation process and also the absence to date of a real alternative to sulfuric acid hydrolysis. Some purely scientific questions also remain open, for example, whether the templated synthesis approach could be extended to the fabrication of semiconductor materials and whether enantioselective catalysis could be carried out in chiral pores. Further studies will help to answer these questions.

The review was written with partial financial support of the Russian Foundation for Basic Research (Project No. 15-43-03022-p_tsentr_a).

References

1. H Zhu, W Luo, P N Ciesielski, Z Fang, J Y Zhu, G Henriksson, M E Himmel, L Hu *Chem. Rev.* **116** 9305 (2016)
2. R M Brown Jr, I M Saxena *Plant Physiol. Biochem.* **38** 57 (2000)
3. V I Kovalenko *Russ. Chem. Rev.* **79** 231 (2010)
4. M Ya Ioelovich *Polym. Sci., Ser. A* **58** 925 (2016)

5. B L Peng, N Dhar, H L Liu, K C Tam *Can. J. Chem. Eng.* **89** 1191 (2011)
6. G Siqueira, J Bras, A Dufresne *Polymers* **2** 728 (2010)
7. D Bondeson, A Mathew, K Oksman *Cellulose* **13** 171 (2006)
8. J Araki, M Wada, S Kuga, T Okano *Colloids Surf., A* **142** 75 (1998)
9. S C Espinosa, T Kuhnt, E J Foster, C Weder *Biomacromolecules* **14** 1223 (2013)
10. J-F Revol, H Bradford, J Giasson, R H Marchessault, D G Gray *Int. J. Biol. Macromol.* **14** 170 (1992)
11. R J Moon, A Martini, J Nairn, J Simonsen, J Youngblood *Chem. Soc. Rev.* **40** 3941 (2011)
12. Y Habibi, L A Lucia, O J Rojas *Chem. Rev.* **110** 3479 (2010)
13. Y Habibi *Chem. Soc. Rev.* **43** 1519 (2014)
14. D Klemm, F Kramer, S Moritz, T Lindström, M Ankerfors, D Gray, A Dorris *Angew. Chem., Int. Ed.* **50** 5438 (2011)
15. S Mondal *Carbohydr. Polym.* **163** 301 (2017)
16. W Y Hamad, T Q Hu *Can. J. Chem. Eng.* **88** 392 (2010)
17. B G Rånby *Discuss. Faraday Soc.* **11** 158 (1951)
18. R H Marchessault, F F Morehead, N M Walter *Nature (London)* **184** 632 (1959)
19. J-F Revol, L Godbout, D G Gray *J. Pulp Pap. Sci.* **24** 146 (1998)
20. M Giese, L K Blusch, M K Khan, M J MacLachlan *Angew. Chem., Int. Ed.* **54** 2888 (2015)
21. S J Eichhorn *Soft Matter* **7** 303 (2011)
22. B Deepa, E Abraham, N Cordeiro, M Mozetic, A P Mathew, K Oksman, M Faria, S Thomas, L A Pothan *Cellulose* **22** 1075 (2015)
23. A García, A Gandini, J Labidi, N Belgacem, J Bras *Ind. Crops Prod.* **93** 26 (2016)
24. J P F Lagerwall, C Schütz, M Salajkova, J-H Noh, J H Park, G Scalia, L Bergstrlm *NPG Asia Mater.* **6** e80 (2014)
25. J Araki, S Kuga *Langmuir* **17** 4493 (2001)
26. J Majoinen, E Kontturi, O Ikkala, D G Gray *Cellulose* **19** 1599 (2012)
27. J Pan, W Hamad, S K Straus *Macromolecules* **43** 3851 (2010)
28. D G Gray, X Mu *Materials* **8** 7873 (2015)
29. J-F Revol, R H Marchessault *Int. J. Biol. Macromol.* **15** 329 (1993)
30. J Araki, M Wada, S Kuga *Langmuir* **17** 21 (2001)
31. L Heux, G Chauve, C Bonini *Langmuir* **16** 8210 (2000)
32. W J Orts, L Godbout, R H Marchessault, J-F Revol *Macromolecules* **31** 5717 (1998)
33. V A Davis *J. Mater. Res.* **26** 140 (2011)
34. X M Dong, T Kimura, J-F Revol, D G Gray *Langmuir* **12** 2076 (1996)
35. Z Hu, E D Cranston, R Ng, R Pelton *Langmuir* **30** 2684 (2014)
36. X M Dong, D G Gray *Langmuir* **13** 2404 (1997)
37. S Beck-Candanedo, D Viet, D G Gray *Cellulose* **13** 629 (2006)
38. S Beck-Candanedo, D Viet, D G Gray *Macromolecules* **40** 3429 (2007)
39. S Beck-Candanedo, D Viet, D G Gray *Langmuir* **22** 8690 (2006)
40. J Araki, M Wada, S Kuga, T Okano *Langmuir* **16** 2413 (2000)
41. Y Habibi, H Chanzy, M R Vignon *Cellulose* **13** 679 (2006)
42. D Viet, S Beck-Candanedo, D G Gray *Cellulose* **14** 109 (2007)
43. H Okura, M Wada, T Serizawa *Chem. Lett.* **43** 601 (2014)
44. L S Blachechen, J P de Mesquita, E L de Paula, F V Pereira, D F S Petri *Cellulose* **20** 1329 (2013)
45. J R Bruckner, A Kuhnhold, C Honorato-Rios, T Schilling, J P F Lagerwall *Langmuir* **32** 9854 (2016)
46. S Elazzouzi-Hafraoui, J-L Putaux, L Heux *J. Phys. Chem. B* **113** 11069 (2009)
47. Q Zhou, H Brumer, T T Teeri *Macromolecules* **42** 5430 (2009)
48. A A Zharov, A I Smirnov, in *Fizicheskaya Entsiklopediya* (Physical Encyclopedia) (Moscow: Bol'shaya Rossiiskaya Entsiklopediya, 1994) Vol. 4, p. 65
49. W Y Hamad, in *Handbook of Nanocellulose and Cellulose Nanocomposites* (Eds H Kargarzadeh, I Ahmad, S Thomas, A Dufresne) (Weinheim: Wiley-VCH, 2017) p. 799
50. V M Dem'yanovich, in *Khimicheskaya Entsiklopediya* (Chemical Encyclopedia) (Editor-in-Chief N S Zefirov) (Moscow: Bol'shaya Rossiiskaya Entsiklopediya, 1998) Vol. 5, p. 273
51. M K Khan, M Giese, M Yu, J A Kelly, W Y Hamad, M J MacLachlan *Angew. Chem., Int. Ed.* **52** 8921 (2013)
52. M Roman, D G Gray *Langmuir* **21** 5555 (2005)
53. D G Gray *Nanomaterials* **6** Art. No. 213 (2016)
54. C C Y Cheung, M Giese, J A Kelly, W Y Hamad, M J MacLachlan *ACS Macro Lett.* **2** 1016 (2013)
55. S Beck, J Bouchard, G Chauve, R Berry *Cellulose* **20** 1401 (2013)
56. T-D Nguyen, W Y Hamad, M J MacLachlan *Chem. Commun.* **49** 11296 (2013)
57. H Tang, B Guo, H Jiang, L Xue, B Li, X Cao, Q Zhang, P Li *Cellulose* **20** 2667 (2013)
58. K J De France, K G Yager, T Hoare, E D Cranston *Langmuir* **32** 7564 (2016)
59. J Sugiyama, H Chanzy, G Maret *Macromolecules* **25** 4232 (1992)
60. E D Cranston, D G Gray *Sci. Technol. Adv. Mater.* **7** 319 (2006)
61. J-F Revol, L Godbout, X-M Dong, D G Gray, H Chanzy, G Maret *Liq. Cryst.* **16** 127 (1994)
62. F Kimura, T Kimura, M Tamura, A Hirai, M Ikuno, F Horii *Langmuir* **21** 2034 (2005)
63. Y Habibi, T Heim, R Douillard *J. Polym. Sci., Part B: Polym. Phys.* **46** 1430 (2008)
64. E E Ureña-Benavides, G Ao, V A Davis, C L Kitchens *Macromolecules* **44** 8990 (2011)
65. M Tatsumi, Y Teramoto, Y Nishio *Cellulose* **22** 2983 (2015)
66. S N Fernandes, Y Geng, S Vignolini, B J Glover, A C Trindade, J P Canejo, P L Almeida, P Brogueira, M H Godinho *Macromol. Chem. Phys.* **214** 25 (2013)
67. M Ličen, B Majaron, J Noh, C Schütz, L Bergström, J Lagerwall, I Drevenšek-Olenik *Cellulose* **23** 3601 (2016)
68. D G Gray, X Mu *ACS Omega* **1** 212 (2016)
69. I Hoeger, O J Rojas, K Efimenko, O D Velev, S S Kelley *Soft Matter* **7** 1957 (2011)
70. T Ebeling, M Paillet, R Borsali, O Diat, A Dufresne, J-Y Cavaille, H Chanzy *Langmuir* **15** 6123 (1999)
71. X Mu, D G Gray *Cellulose* **22** 1103 (2015)
72. A G Dumanli, H M van der Kooij, G Kamita, E Reisner, J J Baumberg, U Steiner, S Vignolini *ACS Appl. Mater. Interfaces* **6** 12302 (2014)
73. A G Dumanli, G Kamita, J Landman, H M van der Kooij, B J Glover, J J Baumberg, U Steiner, S Vignolini *Adv. Opt. Mater.* **2** 646 (2014)
74. B M Weon, J H Je *Phys. Rev. E* **82** 015305 (2010)
75. A Gençer, C Schütz, W Thielemans *Langmuir* **33** 228 (2017)

76. R D Deegan, O Bakajin, T F Dupont, G Huber, S R Nagel, T A Witten *Nature (London)* **389** 827 (1997)
77. R D Deegan *Phys. Rev. E* **61** 475 (2000)
78. P J Yunker, T Still, M A Lohr, A G Yodh *Nature (London)* **476** 308 (2011)
79. P J Yunker, M A Lohr, T Still, A Borodin, D J Durian, A G Yodh *Phys. Rev. Lett.* **110** 035501 (2013)
80. P J Yunker, D J Durian, A G Yodh *Phys. Today* **66** 60 (2013)
81. K Sefiane *Adv. Colloid Interface Sci.* **206** 372 (2014)
82. A Askounis, K Sefiane, V Koutsos, M E R Shanahan *Adv. Colloid Interface Sci.* **222** 44 (2015)
83. S J Kang, V Vandadi, J D Felske, H Masoud *Phys. Rev. E* **94** 063104 (2016)
84. K Uetani, H Yano *ACS Macro Lett.* **1** 651 (2012)
85. K Uetani, H Yano *Soft Matter* **9** 3396 (2013)
86. Mahdi Mashkour, T Kimura, F Kimura, Mehr Mashkour, M Tajvidi *Biomacromolecules* **15** 60 (2014)
87. B Wang, A Walther *ACS Nano* **9** 10637 (2015)
88. H G Yoon, H F Gleeson *J. Phys. D: Appl. Phys.* **40** 3579 (2007)
89. F H Yu, H S Kwok *J. Opt. Soc. Am. A* **16** 2772 (1999)
90. M Giese, M K Khan, W Y Hamad, M J MacLachlan *ACS Macro Lett.* **2** 818 (2013)
91. J A Kelly, A M Shukaliak, C C Y Cheung, K E Shopsowitz, W Y Hamad, M J MacLachlan *Angew. Chem., Int. Ed.* **52** 8912 (2013)
92. K E Shopsowitz, H Qi, W Y Hamad, M J MacLachlan *Nature (London)* **468** 422 (2010)
93. K E Shopsowitz, J A Kelly, W Y Hamad, M J MacLachlan *Adv. Funct. Mater.* **24** 327 (2014)
94. M Giese, L K Blusch, M K Khan, W Y Hamad, M J MacLachlan *Angew. Chem., Int. Ed.* **53** 8880 (2014)
95. K E Shopsowitz, A Stahl, W Y Hamad, M J MacLachlan *Angew. Chem., Int. Ed.* **51** 6886 (2012)
96. K E Shopsowitz, W Y Hamad, M J MacLachlan *Angew. Chem., Int. Ed.* **50** 10991 (2011)
97. J A Kelly, M Giese, K E Shopsowitz, W Y Hamad, M J MacLachlan *Acc. Chem. Res.* **47** 1088 (2014)
98. S H M Mehr, M Giese, H Qi, K E Shopsowitz, W Y Hamad, M J MacLachlan *Langmuir* **29** 12579 (2013)
99. M K Khan, W Y Hamad, M J MacLachlan *Adv. Mater.* **26** 2323 (2014)
100. K E Shopsowitz, W Y Hamad, M J MacLachlan *J. Am. Chem. Soc.* **134** 867 (2012)
101. L L Zhang, X S Zhao *Chem. Soc. Rev.* **38** 2520 (2009)
102. G Chu, J Feng, Y Wang, X Zhang, Y Xu, H Zhang *Dalton Trans.* **43** 15321 (2014)
103. H Qi, K E Shopsowitz, W Y Hamad, M J MacLachlan *J. Am. Chem. Soc.* **133** 3728 (2011)
104. J A Kelly, K E Shopsowitz, J M Ahn, W Y Hamad, M J MacLachlan *Langmuir* **28** 17256 (2012)
105. T-D Nguyen, W Y Hamad, M J MacLachlan *Adv. Funct. Mater.* **24** 777 (2014)
106. J R Capadona, O Van Den Berg, L A Capadona, M Schroeter, S J Rowan, D J Tyler, C Weder *Nat. Nanotechnol.* **2** 765 (2007)